Originally published 28 June 2012; corrected 15 August 2012

www.sciencemag.org/cgi/content/full/science.1225829/DC1

Supplementary Materials for

A Programmable Dual-RNA–Guided DNA Endonuclease in Adaptive Bacterial Immunity

Martin Jinek, Krzysztof Chylinski, Ines Fonfara, Michael Hauer, Jennifer A. Doudna,* Emmanuelle Charpentier*

*To whom correspondence should be addressed. E-mail: doudna@berkeley.edu (J.A.D.); emmanuelle.charpentier@mims.umu.se (E.C.)

Published 28 June 2012 on *Science* Express
DOI: 10.1126/science.1225829

This PDF file includes:

Correction: Formatting errors and typos have been corrected. Additionally, the format of the tables has been revised, and a duplicate entry has been removed from table S2.

SUPPLEMENTARY MATERIALS AND METHODS

Bacterial strains and culture conditions. Table S1 lists the bacterial strains used in the study. *Streptococcus pyogenes*, cultured in THY medium (Todd Hewitt Broth (THB, Bacto, Becton Dickinson) supplemented with 0.2% yeast extract (Oxoid)) or on TSA (trypticase soy agar, BBL, Becton Dickinson) supplemented with 3% sheep blood, was incubated at 37°C in an atmosphere supplemented with 5% CO_2 without shaking. *Escherichia coli*, cultured in Luria-Bertani (LB) medium and agar, was incubated at 37°C with shaking. When required, suitable antibiotics were added to the medium at the following final concentrations: ampicillin, 100 µg/ml for *E. coli*; chloramphenicol, 33 µg/ml for *E. coli*; kanamycin, 25 µg/ml for *E. coli* and 300 µg/ml for *S. pyogenes*. Bacterial cell growth was monitored periodically by measuring the optical density of culture aliquots at 620 nm using a microplate reader (SLT Spectra Reader).

Transformation of bacterial cells. Plasmid DNA transformation into *E. coli* cells was performed according to a standard heat shock protocol (*39*). Transformation of *S. pyogenes* was performed as previously described with some modifications (*40*). The transformation assay performed to monitor in vivo CRISPR/Cas activity on plasmid maintenance was essentially carried out as described previously (*4*). Briefly, electro-competent cells of *S. pyogenes* were equalized to the same cell density and electroporated with 500 ng of plasmid DNA. Every transformation was plated two to three times and the experiment was performed three times independently with different batches of competent cells for statistical analysis. Transformation efficiencies were calculated as CFU (colony forming units) per µg of DNA. Control transformations were performed with sterile water and backbone vector pEC85.

DNA manipulations. DNA manipulations including DNA preparation, amplification, digestion, ligation, purification, agarose gel electrophoresis were performed according to standard techniques (*39*) with minor modifications. Protospacer plasmids for the in vitro cleavage and *S. pyogenes* transformation assays were constructed as described previously (*4*). Additional pUC19-based protospacer plasmids for in vitro cleavage assays were generated by ligating annealed oligonucleotides between digested EcoRI and BamHI sites in pUC19. The GFP gene-containing plasmid has been described previously (*41*). Kits (Qiagen) were used for DNA purification and plasmid preparation. Plasmid mutagenesis was performed using QuikChange® II XL kit (Stratagene) or QuikChange site-directed mutagenesis kit (Agilent). All plasmids used in this study were sequenced at LGC Genomics or the UC Berkeley DNA Sequencing Facility and are listed in Table S2. VBC-Biotech Services, Sigma-Aldrich and Integrated DNA Technologies supplied the synthetic oligonucleotides and RNAs listed in Table S3.

In vitro transcription and purification of RNA. RNA was in vitro transcribed using T7 Flash in vitro Transcription Kit (Epicentre, Illumina company) and PCR-generated DNA templates carrying a T7 promoter sequence. RNA was gel-purified and quality-checked prior to use. The primers used for the preparation of RNA templates from *S. pyogenes* SF370, *Listeria innocua* Clip 11262 and *Neisseria meningitidis* A Z2491 are listed in Table S3.

Protein purification. The sequence encoding Cas9 (residues 1-1368) was PCR-amplified from the genomic DNA of *S. pyogenes* SF370 and inserted into a custom pET-based expression vector using ligation-independent cloning (LIC). The resulting fusion construct contained an N-terminal hexahistidine-maltose binding protein (His_6-MBP) tag, followed by a peptide sequence containing a tobacco etch virus (TEV) protease cleavage site. The protein was expressed in *E. coli* strain BL21 Rosetta 2 (DE3) (EMD Biosciences), grown in 2xTY medium at 18°C for 16 h following induction with 0.2 mM IPTG. The protein was purified by a combination of affinity, ion exchange and size exclusion chromatographic steps. Briefly, cells were lysed in 20 mM Tris pH 8.0, 500 mM NaCl, 1 mM TCEP (supplemented with protease inhibitor cocktail (Roche)) in a homogenizer (Avestin). Clarified lysate was bound in batch to Ni-NTA agarose (Qiagen). The resin was washed extensively with 20 mM Tris pH 8.0, 500 mM NaCl and the bound protein was eluted in 20 mM Tris pH 8.0, 250 mM NaCl, 10% glycerol. The His_6-MBP affinity tag was removed by cleavage with TEV protease, while the protein was dialyzed overnight against 20 mM HEPES pH 7.5, 150 mM KCl, 1 mM TCEP, 10% glycerol. The cleaved Cas9 protein was separated from the fusion tag by purification on a 5 ml SP Sepharose HiTrap column (GE Life Sciences), eluting with a linear gradient of 100 mM – 1 M KCl. The protein was further purified by size exclusion chromatography on a Superdex 200 16/60 column in 20 mM HEPES pH 7.5, 150 mM KCl and 1 mM TCEP. Eluted protein was concentrated to ~8 $mg.ml^{-1}$, flash-frozen in liquid nitrogen and stored at -80°C. Cas9 D10A, H840A and D10A/H840A point mutants were generated using the QuikChange site-directed mutagenesis kit (Agilent) and confirmed by DNA sequencing. The proteins were purified following the same procedure as for the wild-type Cas9 protein.

Cas9 orthologs from *Streptococcus thermophilus* (LMD-9,YP_820832.1), *L. innocua* (Clip11262, NP_472073.1), *Campylobacter jejuni* (*subsp. jejuni* NCTC 11168, YP_002344900.1) and *N. meningitidis* (Z2491, YP_002342100.1) were expressed in BL21 Rosetta (DE3) pLysS cells (Novagen) as His_6-MBP (*N. meningitidis* and *C. jejuni*), His_6-Thioredoxin (*L. innocua*) and His_6-GST (*S. thermophilus*) fusion proteins, and purified essentially as for *S. pyogenes* Cas9 with the following modifications. Due to large amounts of co-purifying nucleic acids, all four Cas9 proteins were purified by an additional heparin sepharose step prior to gel filtration, eluting the bound protein with a linear gradient of 100 mM – 2 M KCl. This successfully removed nucleic acid contamination from the *C. jejuni*, *N. meningitidis* and *L. innocua* proteins, but failed to remove co-purifying nucleic acids from the *S. thermophilus* Cas9 preparation. All proteins were concentrated to 1-8 $mg.ml^{-1}$ in 20 mM HEPES pH 7.5, 150 mM KCl and 1 mM TCEP, flash-frozen in liquid N_2 and stored at -80°C.

Plasmid DNA cleavage assay. Synthetic or in vitro-transcribed tracrRNA and crRNA were pre-annealed prior to the reaction by heating to 95°C and slowly cooling down to room temperature. Native or restriction digest-linearized plasmid DNA (300 ng (~8 nM)) was incubated for 60 min at 37°C with purified Cas9 protein (50-500 nM) and tracrRNA:crRNA duplex (50-500 nM, 1:1) in a Cas9 plasmid cleavage buffer (20 mM HEPES pH 7.5, 150 mM KCl, 0.5 mM DTT, 0.1 mM EDTA) with or without 10 mM $MgCl_2$. The reactions were stopped with 5X DNA loading buffer containing 250 mM EDTA, resolved by 0.8 or 1% agarose gel electrophoresis and visualized by ethidium bromide

staining. For the Cas9 mutant cleavage assays, the reactions were stopped with 5X SDS loading buffer (30% glycerol, 1.2% SDS, 250 mM EDTA) prior to loading on the agarose gel.

Metal-dependent cleavage assay. Protospacer 2 plasmid DNA (5 nM) was incubated for 1 h at 37°C with Cas9 (50 nM) pre-incubated with 50 nM tracrRNA:crRNA-sp2 in cleavage buffer (20 mM HEPES pH 7.5, 150 mM KCl, 0.5 mM DTT, 0.1 mM EDTA) supplemented with 1, 5 or 10 mM $MgCl_2$, 1 or 10 mM of $MnCl_2$, $CaCl_2$, $ZnCl_2$, $CoCl_2$, $NiSO_4$ or $CuSO_4$. The reaction was stopped by adding 5X SDS loading buffer (30% glycerol, 1.2% SDS, 250 mM EDTA), resolved by 1% agarose gel electrophoresis and visualized by ethidium bromide staining.

Single-turnover assay. Cas9 (25 nM) was pre-incubated 15 min at 37°C in cleavage buffer (20 mM HEPES pH 7.5, 150 mM KCl, 10 mM $MgCl_2$, 0.5 mM DTT, 0.1 mM EDTA) with duplexed tracrRNA:crRNA-sp2 (25 nM, 1:1) or both RNAs (25 nM) not pre-annealed and the reaction was started by adding protospacer 2 plasmid DNA (5 nM). The reaction mix was incubated at 37°C. At defined time intervals, samples were withdrawn from the reaction, 5X SDS loading buffer (30% glycerol, 1.2% SDS, 250 mM EDTA) was added to stop the reaction and the cleavage was monitored by 1% agarose gel electrophoresis and ethidium bromide staining. The same was done for the single turnover kinetics without pre-incubation of Cas9 and RNA, where protospacer 2 plasmid DNA (5 nM) was mixed in cleavage buffer with duplex tracrRNA:crRNA-sp2 (25 nM) or both RNAs (25 nM) not pre-annealed, and the reaction was started by addition of Cas9 (25 nM). Percentage of cleavage was analyzed by densitometry and the average of three independent experiments was plotted against time. The data were fit by nonlinear regression analysis and the cleavage rates (k_{obs} [min^{-1}]) were calculated.

Multiple-turnover assay. Cas9 (1 nM) was pre-incubated for 15 min at 37°C in cleavage buffer (20 mM HEPES pH 7.5, 150 mM KCl, 10 mM $MgCl_2$, 0.5 mM DTT, 0.1 mM EDTA) with pre-annealed tracrRNA:crRNA-sp2 (1 nM, 1:1). The reaction was started by addition of protospacer 2 plasmid DNA (5 nM). At defined time intervals, samples were withdrawn and the reaction was stopped by adding 5X SDS loading buffer (30% glycerol, 1.2% SDS, 250 mM EDTA). The cleavage reaction was resolved by 1% agarose gel electrophoresis, stained with ethidium bromide and the percentage of cleavage was analyzed by densitometry. The results of four independent experiments were plotted against time (min).

Oligonucleotide DNA cleavage assay. DNA oligonucleotides (10 pmol) were radiolabeled by incubating with 5 units T4 polynucleotide kinase (New England Biolabs) and ~3–6 pmol (~20–40 mCi) [γ-32P]-ATP (Promega) in 1X T4 polynucleotide kinase reaction buffer at 37°C for 30 min, in a 50 μL reaction. After heat inactivation (65°C for 20 min), reactions were purified through an Illustra MicroSpin G-25 column (GE Healthcare) to remove unincorporated label. Duplex substrates (100 nM) were generated by annealing labeled oligonucleotides with equimolar amounts of unlabeled complementary oligonucleotide at 95°C for 3 min, followed by slow cooling to room temperature. For cleavage assays, tracrRNA and crRNA were annealed by heating to 95°C for 30 s, followed by slow cooling to room temperature. Cas9 (500 nM final concentration) was

pre-incubated with the annealed tracrRNA:crRNA duplex (500 nM) in cleavage assay buffer (20 mM HEPES pH 7.5, 100 mM KCl, 5 mM $MgCl_2$, 1 mM DTT, 5% glycerol) in a total volume of 9 μl. Reactions were initiated by the addition of 1 μl target DNA (10 nM) and incubated for 1 h at 37°C. Reactions were quenched by the addition of 20 μl of loading dye (5 mM EDTA, 0.025% SDS, 5% glycerol in formamide) and heated to 95°C for 5 min. Cleavage products were resolved on 12% denaturing polyacrylamide gels containing 7 M urea and visualized by phosphorimaging (Storm, GE Life Sciences). Cleavage assays testing PAM requirements (Fig. 4B) were carried out using DNA duplex substrates that had been pre-annealed and purified on an 8% native acrylamide gel, and subsequently radiolabeled at both 5' ends. The reactions were set-up and analyzed as above.

Electrophoretic mobility shift assays. Target DNA duplexes were formed by mixing of each strand (10 nmol) in deionized water, heating to 95°C for 3 min and slow cooling to room temperature. All DNAs were purified on 8% native gels containing 1X TBE. DNA bands were visualized by UV shadowing, excised, and eluted by soaking gel pieces in DEPC-treated H_2O. Eluted DNA was ethanol precipitated and dissolved in DEPC-treated H_2O. DNA samples were 5' end labeled with [γ-32P]-ATP using T4 polynucleotide kinase (New England Biolabs) for 30 min at 37°C. PNK was heat denatured at 65°C for 20 min, and unincorporated radiolabel was removed using an Illustra MicroSpin G-25 column (GE Healthcare). Binding assays were performed in buffer containing 20 mM HEPES pH 7.5, 100 mM KCl, 5 mM $MgCl_2$, 1 mM DTT and 10% glycerol in a total volume of 10 μl. Cas9 D10A/H840A double mutant was programmed with equimolar amounts of pre-annealed tracrRNA:crRNA duplex and titrated from 100 pM to 1 μM. Radiolabeled DNA was added to a final concentration of 20 pM. Samples were incubated for 1 h at 37°C and resolved at 4°C on an 8% native polyacrylamide gel containing 1X TBE and 5 mM $MgCl_2$. Gels were dried and DNA visualized by phosphorimaging.

In silico analysis of DNA and protein sequences. Vector NTI package (Invitrogen) was used for DNA sequence analysis (Vector NTI) and comparative sequence analysis of proteins (AlignX).

In silico modeling of RNA structure and co-folding. In silico predictions were performed using the Vienna RNA package algorithms (*42, 43*). RNA secondary structures and co-folding models were predicted with RNAfold and RNAcofold, respectively and visualized with VARNA (*44*).

SUPPLEMENTARY FIGURES

Figure S1

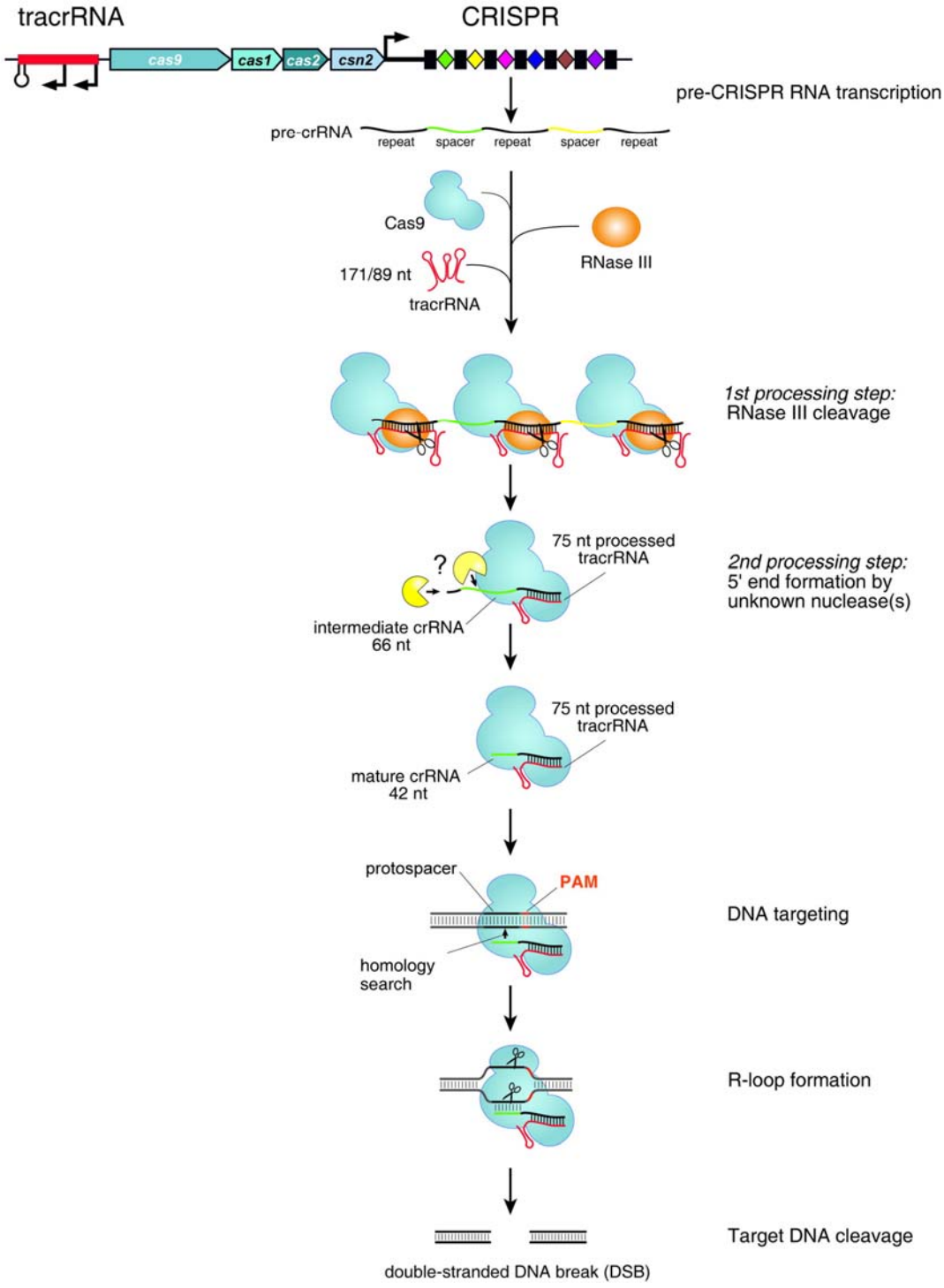

Fig. S1. The type II RNA-mediated CRISPR/Cas immune pathway. The expression and interference steps are represented in the drawing. The type II CRISPR/Cas loci are composed of an operon of four genes (blue) encoding the proteins Cas9, Cas1, Cas2 and Csn2, a CRISPR array consisting of a leader sequence followed by identical repeats (black rectangles) interspersed with unique genome-targeting spacers (colored diamonds) and a sequence encoding the *trans*-activating tracrRNA (red). Represented here is the type II CRISPR/Cas locus of *S. pyogenes* SF370 (Accession number NC_002737) (*4*). Experimentally confirmed promoters and transcriptional terminator in this locus are indicated (*4*). The CRISPR array is transcribed as a precursor CRISPR RNA (pre-crRNA) molecule that undergoes a maturation process specific to the type II systems (*4*). In *S. pyogenes* SF370, tracrRNA is transcribed as two primary transcripts of 171 and 89 nt in length that have complementarity to each repeat of the pre-crRNA. The first processing event involves pairing of tracrRNA to pre-crRNA, forming a duplex RNA that is recognized and cleaved by the housekeeping endoribonuclease RNase III (orange) in the presence of the Cas9 protein. RNase III-mediated cleavage of the duplex RNA generates a 75-nt processed tracrRNA and a 66-nt intermediate crRNAs consisting of a central region containing a sequence of one spacer, flanked by portions of the repeat sequence. A second processing event, mediated by unknown ribonuclease(s), leads to the formation of mature crRNAs of 39 to 42 nt in length consisting of 5'-terminal spacer-derived guide sequence and repeat-derived 3'-terminal sequence. Following the first and second processing events, mature tracrRNA remains paired to the mature crRNAs and bound to the Cas9 protein. In this ternary complex, the dual tracrRNA:crRNA structure acts as guide RNA that directs the endonuclease Cas9 to the cognate target DNA. Target recognition by the Cas9-tracrRNA:crRNA complex is initiated by scanning the invading DNA molecule for homology between the protospacer sequence in the target DNA and the spacer-derived sequence in the crRNA. In addition to the DNA protospacer-crRNA spacer complementarity, DNA targeting requires the presence of a short motif (NGG, where N can be any nucleotide) adjacent to the protospacer (protospacer adjacent motif - PAM). Following pairing between the dual-RNA and the protospacer sequence, an R-loop is formed and Cas9 subsequently introduces a double-stranded break (DSB) in the DNA. Cleavage of target DNA by Cas9 requires two catalytic domains in the protein. At a specific site relative to the PAM, the HNH domain cleaves the complementary strand of the DNA while the RuvC-like domain cleaves the noncomplementary strand.

Figure S2

A

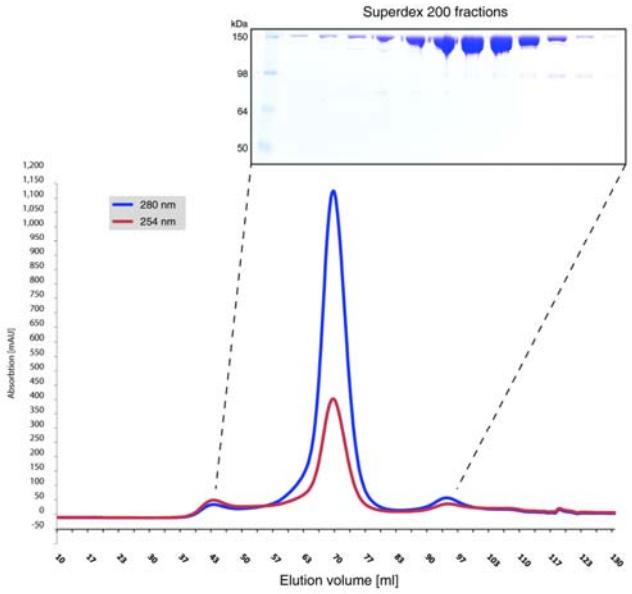

B

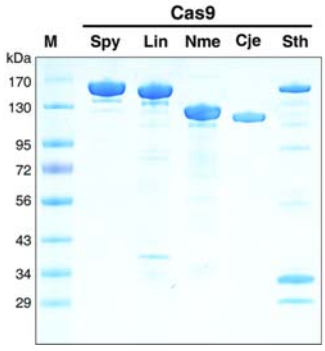

Fig. S2. Purification of Cas9 nucleases. (A) *S. pyogenes* Cas9 was expressed in *E. coli* as a fusion protein containing an N-terminal His_6-MBP tag and purified by a combination of affinity, ion exchange and size exclusion chromatographic steps. The affinity tag was removed by TEV protease cleavage following the affinity purification step. Shown is a chromatogram of the final size exclusion chromatography step on a Superdex 200 (16/60) column. Cas9 elutes as a single monomeric peak devoid of contaminating nucleic acids, as judged by the ratio of absorbances at 280 and 260 nm. Inset; eluted fractions were resolved by SDS-PAGE on a 10% polyacrylamide gel and stained with SimplyBlue Safe Stain (Invitrogen). **(B)** SDS-PAGE analysis of purified Cas9 orthologs. Cas9 orthologs were purified as described in Supplementary Materials and Methods. 2.5 μg of each purified Cas9 were analyzed on a 4-20% gradient polyacrylamide gel and stained with SimplyBlue Safe Stain.

Figure S3

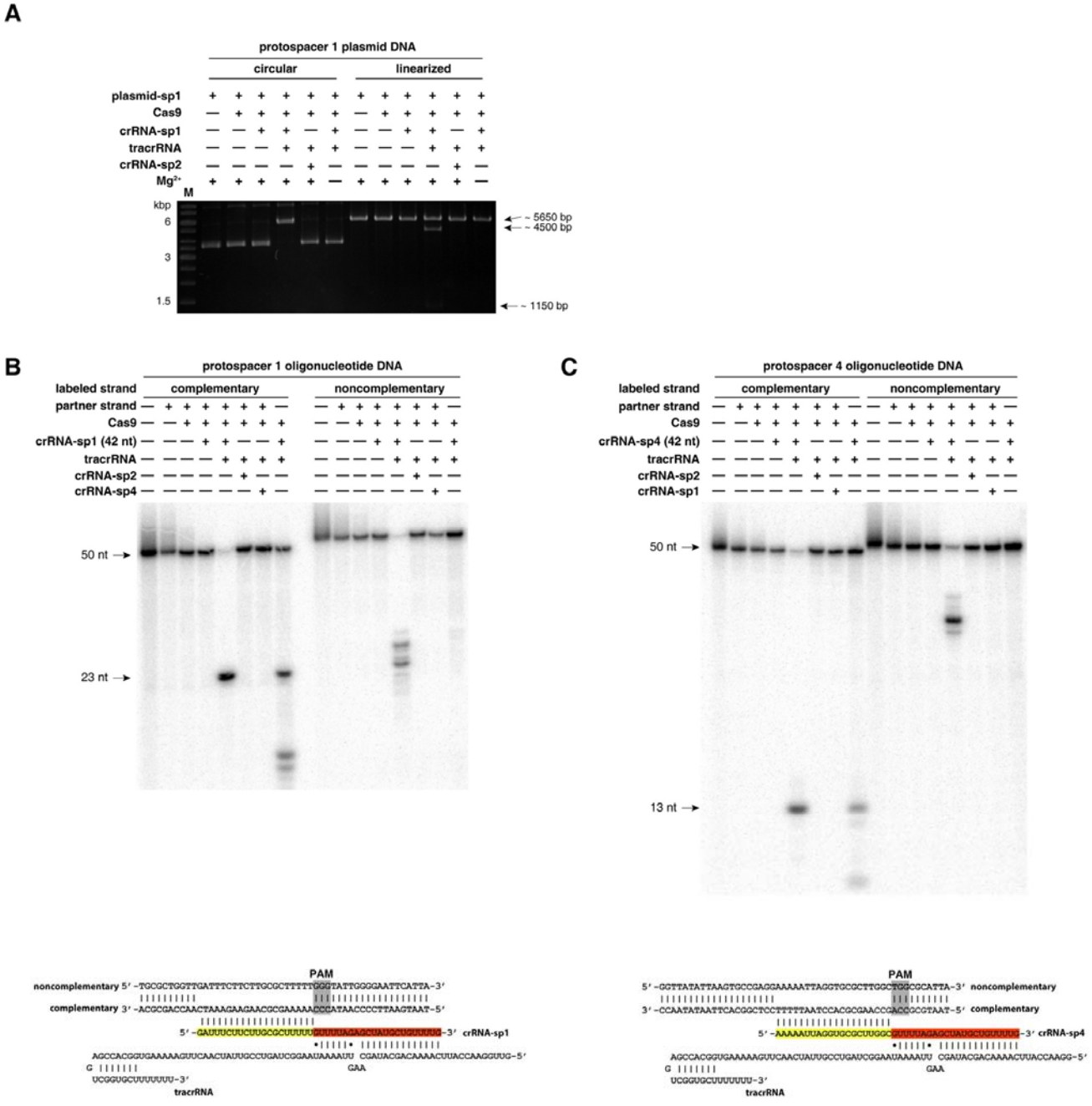

Fig. S3. Cas9 guided by dual-tracrRNA:crRNA cleaves protospacer plasmid and oligonucleotide DNA. See Fig. 1. The protospacer 1 sequence originates from *S. pyogenes* SF370 (M1) SPy_0700, target of *S. pyogenes* SF370 crRNA-sp1 (*4*). Here, the protospacer 1 sequence was manipulated by changing the PAM from a nonfunctional sequence (TTG) to a functional one (TGG). The protospacer 4 sequence originates from *S. pyogenes* MGAS10750 (M4) MGAS10750_Spy1285, target of *S. pyogenes* SF370 crRNA-sp4 (*4*). **(A)** Protospacer 1 plasmid DNA cleavage guided by cognate tracrRNA:crRNA

duplexes. The cleavage products were resolved by agarose gel electrophoresis and visualized by ethidium bromide staining. M, DNA marker; fragment sizes in base pairs are indicated. **(B)** Protospacer 1 oligonucleotide DNA cleavage guided by cognate tracrRNA:crRNA-sp1 duplex. The cleavage products were resolved by denaturating polyacrylamide gel electrophoresis and visualized by phosphorimaging. Fragment sizes in nucleotides are indicated. **(C)** Protospacer 4 oligonucleotide DNA cleavage guided by cognate tracrRNA:crRNA-sp4 duplex. The cleavage products were resolved by denaturating polyacrylamide gel electrophoresis and visualized by phosphorimaging. Fragment sizes in nucleotides are indicated. **(A, B, C)** Experiments in (A) were performed as in Fig. 1A; in (B) and in (C) as in Fig. 1B. **(B, C)** A schematic of the tracrRNA:crRNA-target DNA interaction is shown below. The regions of crRNA complementarity to tracrRNA and the protospacer DNA are represented in orange and yellow, respectively. The PAM sequence is indicated in grey.

Figure S4

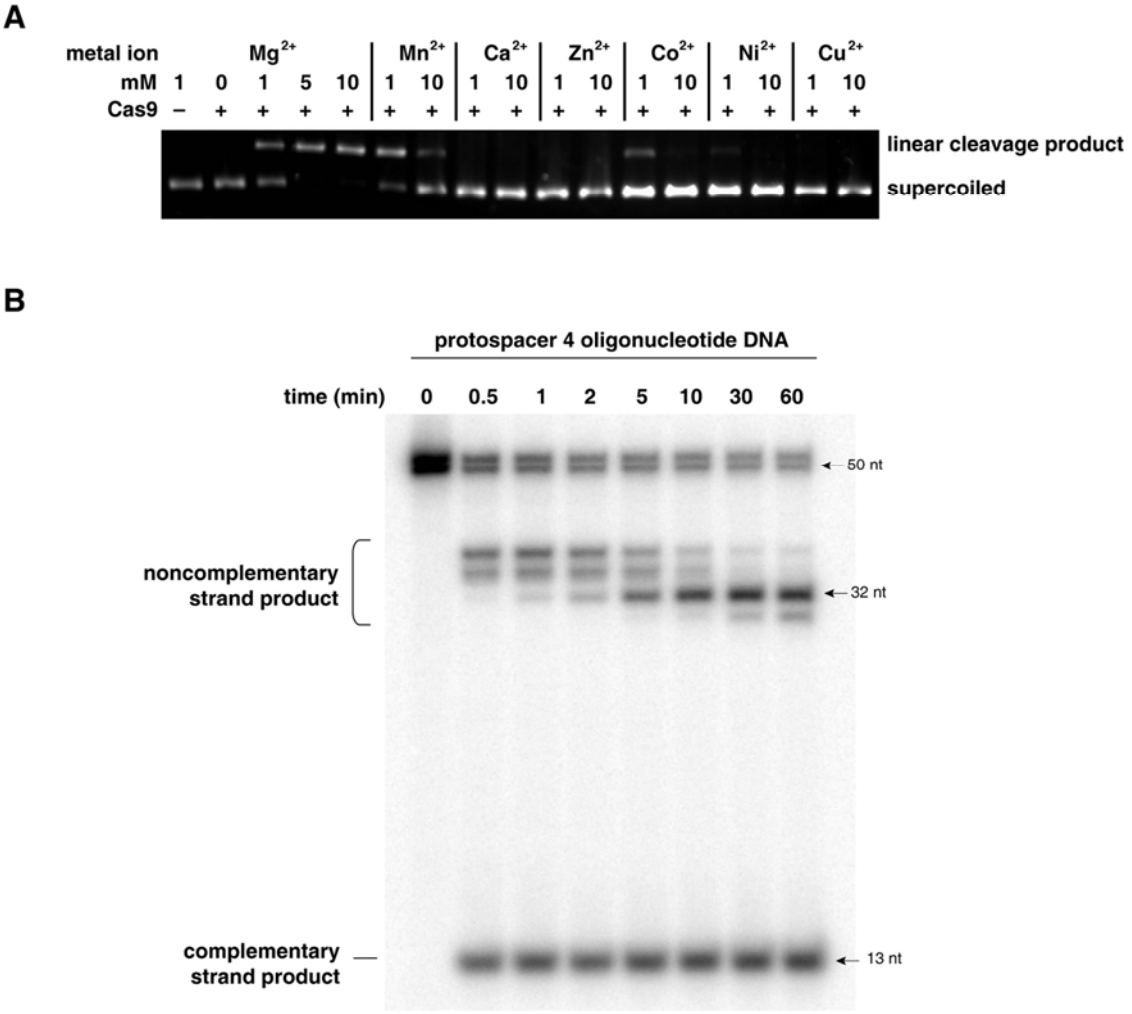

Fig. S4. Cas9 is a Mg^{2+}-dependent endonuclease with 3'-5' exonuclease activity. See Fig. 1. **(A)** Protospacer 2 plasmid DNA was incubated with Cas9 complexed with tracrRNA:crRNA-sp2 in the presence of different concentrations of Mg^{2+}, Mn^{2+}, Ca^{2+}, Zn^{2+}, Co^{2+}, Ni^{2+} or Cu^{2+}. The cleavage products were resolved by agarose gel electrophoresis and visualized by ethidium bromide staining. Plasmid forms are indicated. **(B)** A protospacer 4 oligonucleotide DNA duplex containing a PAM motif was annealed and gel-purified prior to radiolabeling at both 5' ends. The duplex (10 nM final concentration) was incubated with Cas9 programmed with tracrRNA (nucleotides 23-89) and crRNA-sp4 (500 nM final concentration, 1:1). At indicated time points (min), 10 μl aliquots of the cleavage reaction were quenched with formamide buffer containing 0.025% SDS and 5 mM EDTA, and analyzed by denaturing polyacrylamide gel electrophoresis as in Fig. 1B. Sizes in nucleotides are indicated.

Figure S5

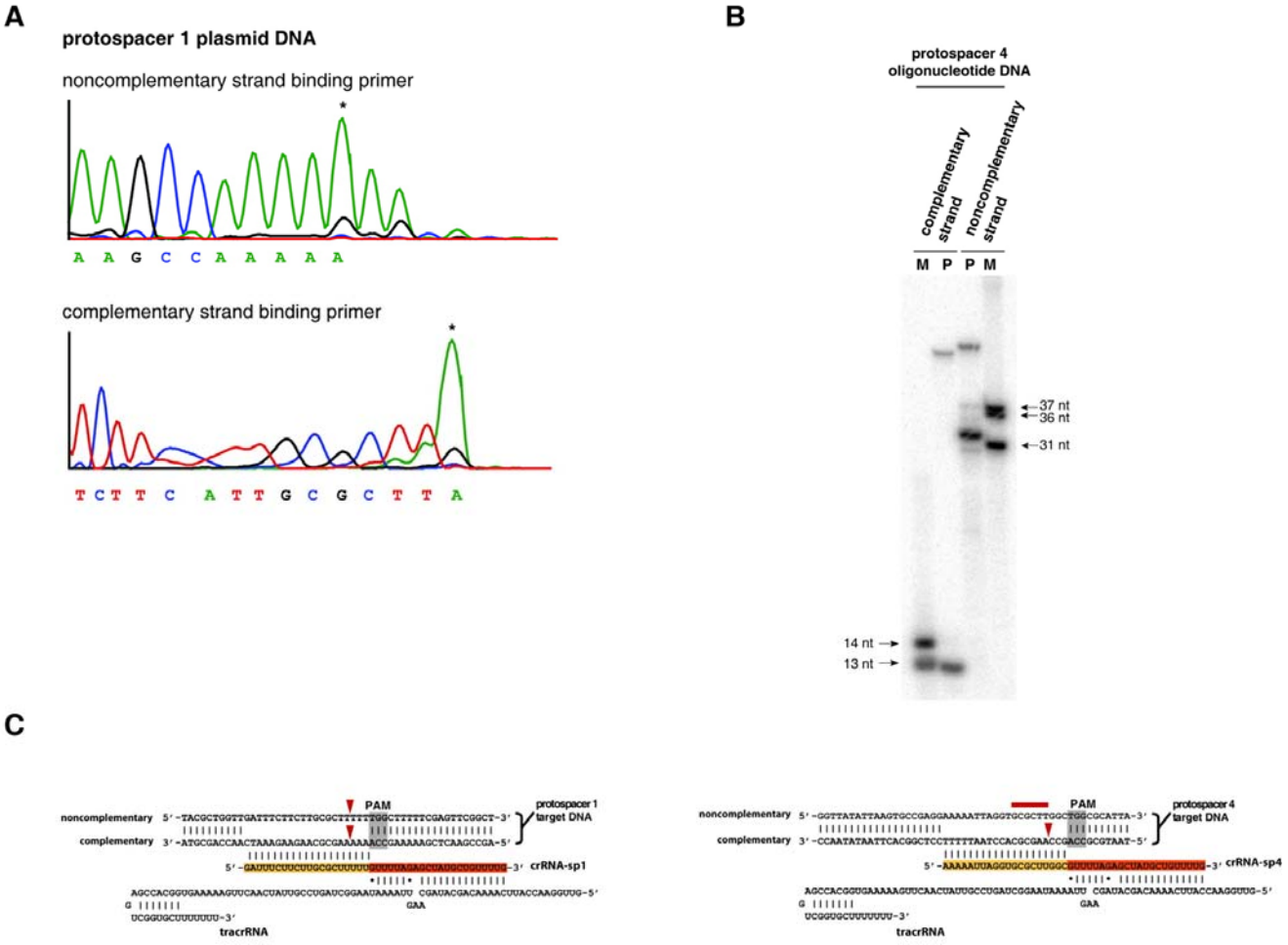

Fig. S5. Dual-tracrRNA:crRNA directed Cas9 cleavage of target DNA is site-specific. See Fig. 1 and fig. S3. **(A)** Mapping of protospacer 1 plasmid DNA cleavage. Cleavage products from fig. S3A were analyzed by sequencing as in Fig. 1C. Note that the 3' terminal A overhang (asterisk) is an artifact of the sequencing reaction. **(B)** Mapping of protospacer 4 oligonucleotide DNA cleavage. Cleavage products from fig. S3C were analyzed by denaturing polyacrylamide gel electrophoresis alongside 5' end-labeled oligonucleotide size markers derived from the complementary and noncomplementary strands of the protospacer 4 duplex DNA. M, marker; P, cleavage product. Fragment sizes in nucleotides are indicated. **(C)** Schematic representations of tracrRNA, crRNA-sp1 and protospacer 1 DNA sequences (left) and tracrRNA, crRNA-sp4 and protospacer 4 DNA sequences (right). tracrRNA:crRNA forms a dual-RNA structure directed to complementary protospacer DNA through crRNA-protospacer DNA pairing. The regions of crRNA complementary to tracrRNA and the protospacer DNA are represented in orange and yellow, respectively. The cleavage sites in the complementary and noncomplementary DNA strands mapped in (A) (left) and (B) (right) are represented with red arrows (A and B, complementary strand) and a red thick line (B, noncomplementary strand) above the sequences, respectively.

Figure S6

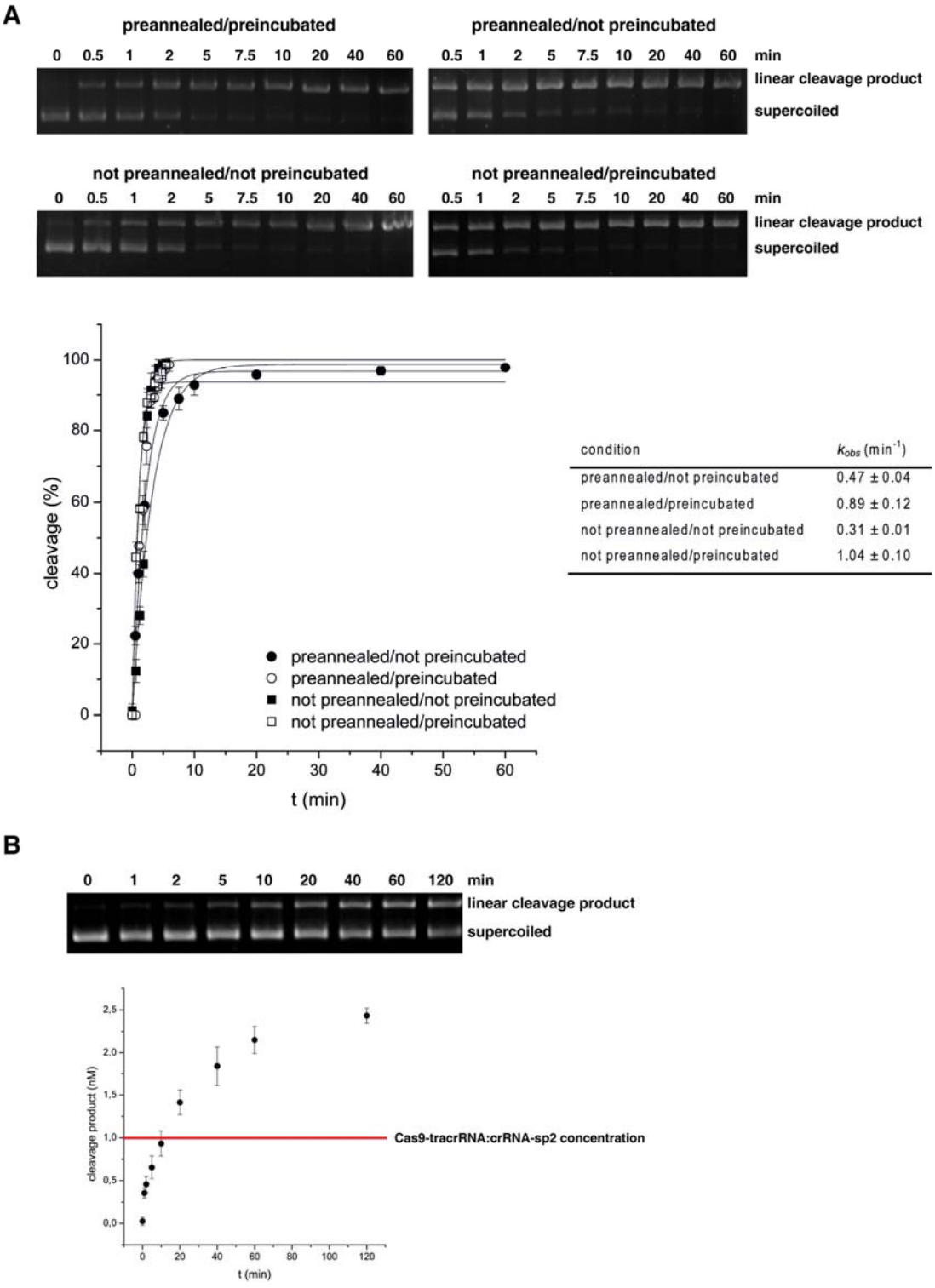

Fig. S6. Dual-tracrRNA:crRNA directed Cas9 cleavage of target DNA is fast and efficient. See Fig. 1. **(A)** Single turnover kinetics of Cas9 under different RNA pre-annealing and protein-RNA pre-incubation conditions. Protospacer 2

plasmid DNA was incubated with either Cas9 pre-incubated with pre-annealed tracrRNA:crRNA-sp2 (○), Cas9 not pre-incubated with pre-annealed tracrRNA:crRNA-sp2 (●), Cas9 pre-incubated with not pre-annealed tracrRNA and crRNA-sp2 (□) or Cas9 not pre-incubated with not pre-annealed RNAs (■). The cleavage activity was monitored in a time-dependent manner and analyzed by agarose gel electrophoresis followed by ethidium bromide staining. The average percentage of cleavage from three independent experiments is plotted against the time (min) and fitted with a nonlinear regression. The calculated cleavage rates (k_{obs}) are shown in the table on the right. The results suggest that the binding of Cas9 to the RNAs is not rate-limiting under the conditions tested. Plasmid forms are indicated. The obtained k_{obs} values are comparable to those of restriction endonucleases which are typically of the order of 1-10 min^{-1} (*45-47*). **(B)** Cas9 is a multiple turnover endonuclease. Cas9 loaded with duplexed tracrRNA:crRNA-sp2 (1 nM, 1:1:1 – indicated with red line on the graph) was incubated with a 5-fold excess of native protospacer 2 plasmid DNA. Cleavage was monitored by withdrawing samples from the reaction at defined time intervals (0 to 120 min) followed by agarose gel electrophoresis analysis (top) and determination of cleavage product amount (nM) (bottom). Standard deviations of three independent experiments are indicated. In the time interval investigated, 1 nM Cas9 was able to cleave ~2.5 nM plasmid DNA.

Figure S7

Fig. S7. Cas9 contains two nuclease domains: HNH (McrA-like) and RuvC-like (N-terminal RNase H fold) resolvase. See Fig. 2. The amino-acid sequence of Cas9 from *S. pyogenes* SF370 (Accession number NC_002737) is represented. The three predicted RuvC-like motifs and the predicted HNH motif are shaded light blue and purple, respectively. Residues Asp10 and His840, which were substituted by Ala in this study are shown in red and highlighted by a red asterisk above the sequence. Underlined residues are highly conserved among Cas9 proteins from different species. Note that in a previous study and based on computational predictions, Makarova *et al*. (*23*) predicted coupling of the two nuclease-like activities, which is now confirmed experimentally in the present study (Fig. 2 and fig. S8).

Figure S8

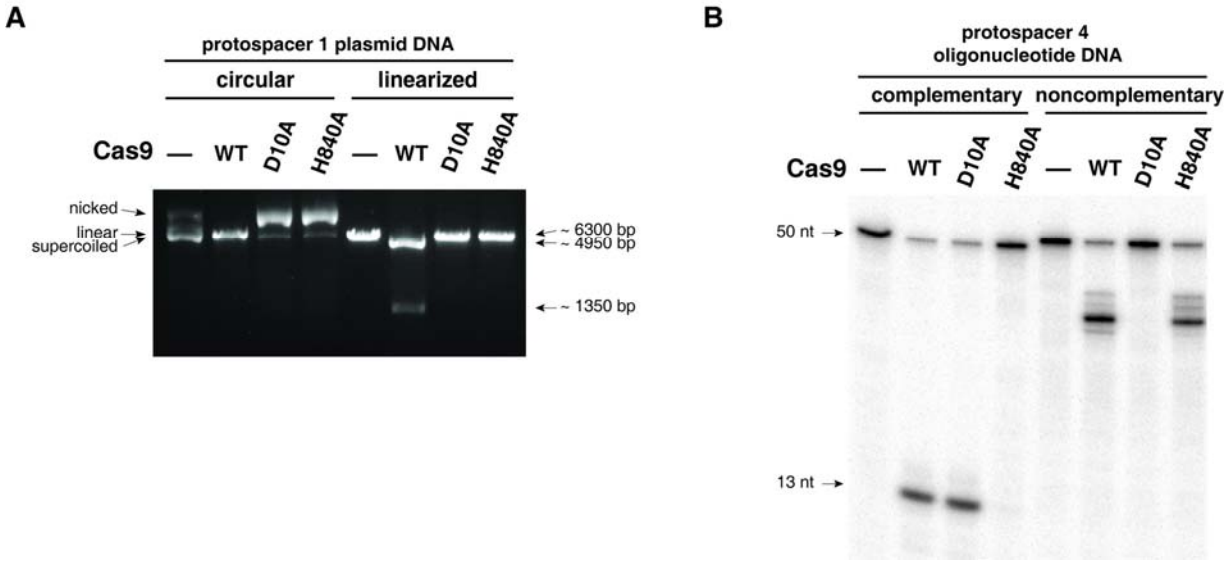

Fig. S8. The HNH and RuvC-like domains of Cas9 direct cleavage of the complementary and noncomplementary DNA strand, respectively. See Fig. 2. Protospacer DNA cleavage by cognate tracrRNA:crRNA-directed Cas9 mutants containing mutations in the HNH or RuvC-like domain. **(A)** Protospacer 1 plasmid DNA cleavage. The experiment was performed as in Fig. 2A. Plasmid DNA conformations and sizes in base pairs are indicated. **(B)** Protospacer 4 oligonucleotide DNA cleavage. The experiment was performed as in Fig. 2B. Sizes in nucleotides are indicated.

Figure S9

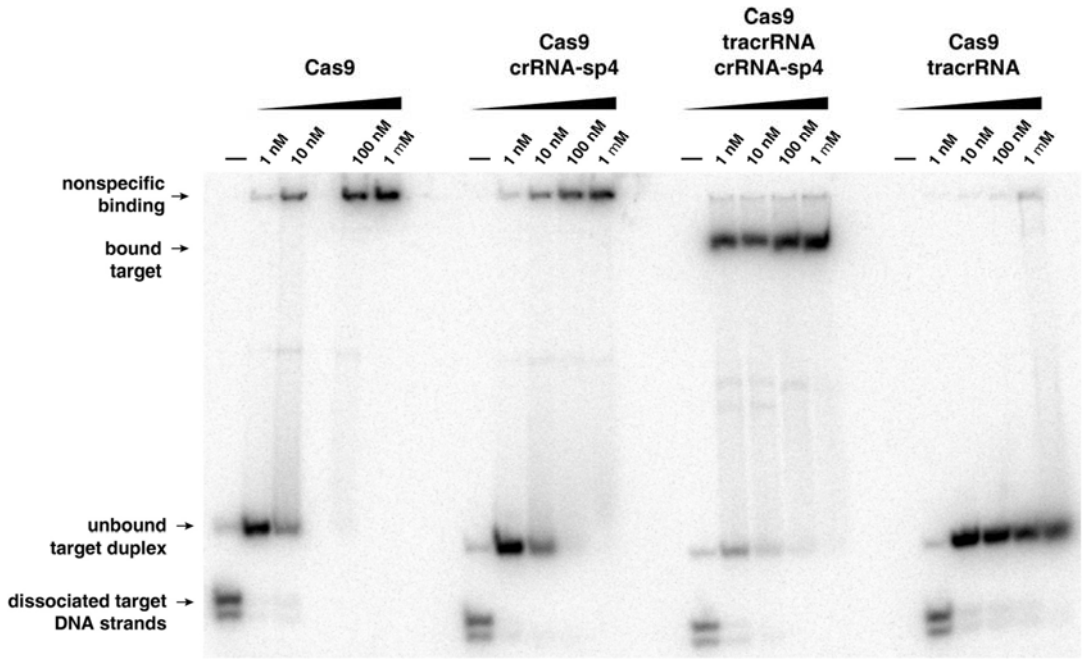

Fig. S9. tracrRNA is required for target DNA recognition. Electrophoretic mobility shift assays were performed using protospacer 4 target DNA duplex and Cas9 (containing nuclease domain inactivating mutations D10A and H840) alone or in the presence of crRNA-sp4, tracrRNA (75nt), or both. The target DNA duplex was radiolabeled at both 5' ends. Cas9 (D10/H840A) and complexes were titrated from 1 nM to 1 μM. Binding was analyzed by 8% native polyacrylamide gel electrophoresis and visualized by phosphorimaging.

Note that Cas9 alone binds target DNA with moderate affinity. This binding is unaffected by the addition of crRNA, suggesting that this represents sequence nonspecific interaction with the dsDNA. Furthermore, this interaction can be outcompeted by tracrRNA alone in the absence of crRNA. In the presence of both crRNA and tracrRNA, target DNA binding is substantially enhanced and yields a species with distinct electrophoretic mobility, indicative of specific target DNA recognition.

Figure S10

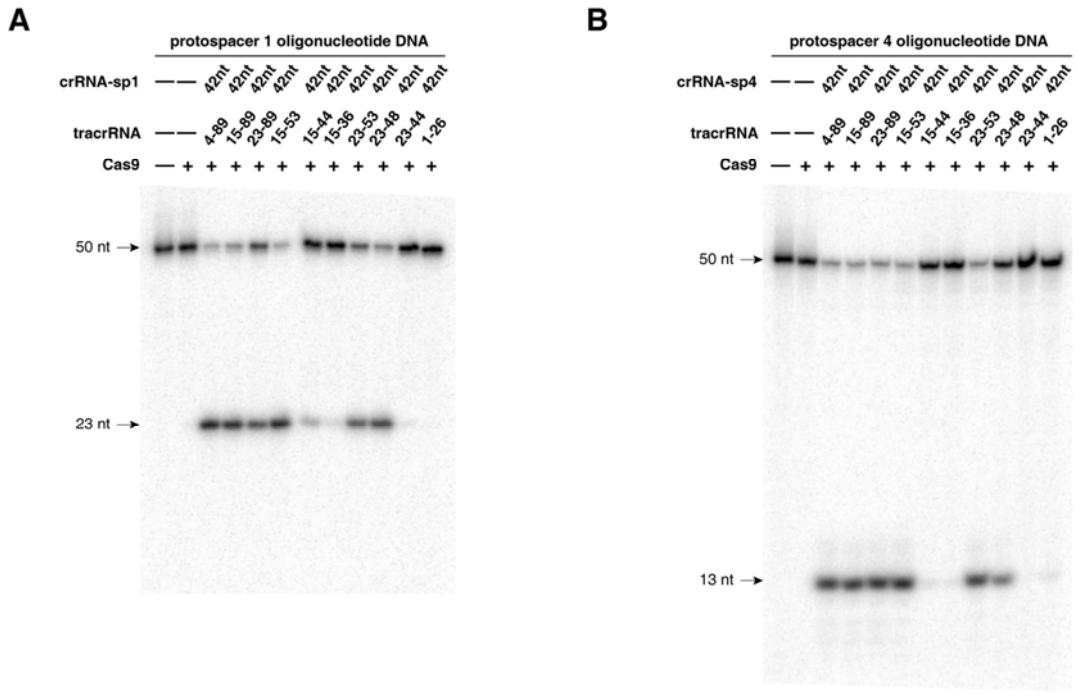

Fig. S10. Minimal region of tracrRNA capable of guiding dual-tracrRNA:crRNA directed cleavage of target DNA. See Fig. 3. A fragment of tracrRNA encompassing a part of the crRNA paired region and a portion of the downstream region is sufficient to direct cleavage of protospacer oligonucleotide DNA by Cas9. **(A)** Protospacer 1 oligonucleotide DNA cleavage and **(B)** Protospacer 4 oligonucleotide DNA cleavage by Cas9 guided with a mature cognate crRNA and various tracrRNA fragments. **(A, B)** Sizes in nucleotides are indicated.

Figure S11

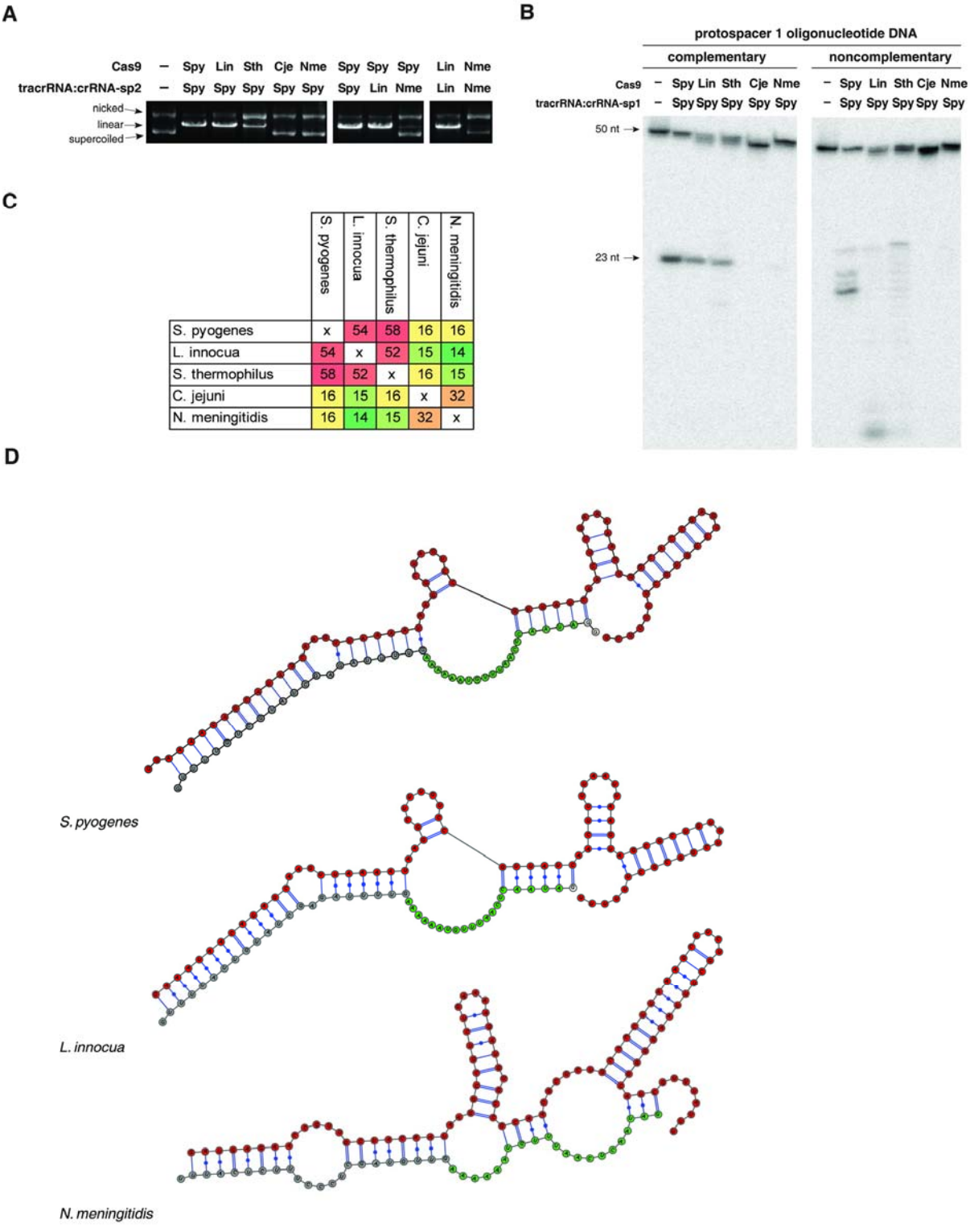

Fig. S11. Dual-tracrRNA:crRNA guided target DNA cleavage by Cas9 is species specific. See Fig. 3. Like Cas9 from *S. pyogenes*, the closely related Cas9 orthologs from the Gram-positive bacteria *L. innocua* and *S. thermophilus* cleave protospacer

DNA when targeted by tracrRNA:crRNA from *S. pyogenes*. However, under the same conditions, DNA cleavage by the less closely related Cas9 orthologs from the Gram-negative bacteria *C. jejuni* and *N. meningitidis* is not observed. Spy, *S. pyogenes* SF370 (Accession Number NC_002737); Sth, *S. thermophilus* LMD-9 (STER_1477 Cas9 ortholog; Accession Number NC_008532); Lin, *L. innocua* Clip11262 (Accession Number NC_003212); Cje, *C. jejuni* NCTC 11168 (Accession Number NC_002163); Nme, *N. meningitidis* A Z2491 (Accession Number NC_003116). **(A)** Cleavage of protospacer plasmid DNA. Protospacer 2 plasmid DNA (300 ng) was subjected to cleavage by different Cas9 orthologs (500 nM) guided by hybrid tracrRNA:crRNA-sp2 duplexes (500 nM, 1:1) from different species. To design the RNA duplexes, we predicted tracrRNA sequences from *L. innocua* and *N. meningitidis* based on previously published Northern blot data *(4)*. The dual-hybrid RNA duplexes consist of species-specific tracrRNA and a heterologous crRNA. The heterologous crRNA sequence was engineered to contain *S. pyogenes* DNA-targeting sp2 sequence at the 5' end fused to *L. innocua* or *N. meningitidis* tracrRNA-binding repeat sequence at the 3' end. Cas9 orthologs from *S. thermophilus* and *L. innocua,* but not from *N. meningitidis* or *C. jejuni*, can be guided by *S. pyogenes* tracrRNA:crRNA-sp2 to cleave protospacer 2 plasmid DNA, albeit with slightly decreased efficiency. Similarly, the hybrid *L. innocua* tracrRNA:crRNA-sp2 can guide *S. pyogenes* Cas9 to cleave the target DNA with high efficiency, whereas the hybrid *N. meningitidis* tracrRNA:crRNA-sp2 triggers only slight DNA cleavage activity by *S. pyogenes* Cas9. As controls, *N. meningitidis* and *L. innocua* Cas9 orthologs cleave protospacer 2 plasmid DNA when guided by the cognate hybrid tracrRNA:crRNA-sp2. Note that as mentioned above, the tracrRNA sequence of *N. meningitidis* is predicted only and has not yet been confirmed by RNA sequencing. Therefore, the low efficiency of cleavage could be the result of either low activity of the Cas9 orthologs or the use of a nonoptimally designed tracrRNA sequence. **(B)** Cleavage of protospacer oligonucleotide DNA. 5'-end radioactively labeled complementary strand oligonucleotide (10 nM) pre-annealed with unlabeled noncomplementary strand oligonucleotide (protospacer 1) (10 nM) (left) or 5'-end radioactively labeled noncomplementary strand oligonucleotide (10 nM) pre-annealed with unlabeled complementary strand oligonucleotide (10 nM) (right) (protospacer 1) was subjected to cleavage by various Cas9 orthologs (500 nM) guided by tracrRNA:crRNA-sp1 duplex from *S. pyogenes* (500 nM, 1:1). Cas9 orthologs from *S. thermophilus* and *L. innocua*, but not from *N. meningitidis* or *C. jejuni* can be guided by *S. pyogenes* cognate dual-RNA to cleave the protospacer oligonucleotide DNA, albeit with decreased efficiency. Note that the cleavage site on the complementary DNA strand is identical for all three orthologs. Cleavage of the noncomplementary strand occurs at distinct positions. **(C)** Amino acid sequence identity of Cas9 orthologs. *S. pyogenes*, *S. thermophilus* and *L. innocua* Cas9 orthologs share high percentage of amino acid identity. In contrast, the *C. jejuni* and *N. meningitidis* Cas9 proteins differ in sequence and length (~300-400 amino acids shorter). **(D)** Co-foldings of engineered species-specific heterologous crRNA sequences with the corresponding tracrRNA orthologs from *S. pyogenes* (experimentally confirmed, (*4*)), *L. innocua* (predicted) or *N. meningitidis* (predicted). Red, tracrRNA; green, crRNA spacer 2 fragment; grey, crRNA repeat fragment. *L. innocua* and *S. pyogenes* hybrid tracrRNA:crRNA-sp2 duplexes share very similar structural characteristics, albeit distinct from the *N. meningitidis* hybrid tracrRNA:crRNA. Together with the cleavage data described above in (A) and (B),

the co-folding predictions would indicate that the species-specificity cleavage of target DNA by Cas9-tracrRNA:crRNA is dictated by a still unknown structural feature in the tracrRNA:crRNA duplex that is recognized specifically by a cognate Cas9 ortholog. We predict that the species-specificity of cleavage observed in (A) and (B) occurs at the level of binding of Cas9 to dual-tracrRNA:crRNA. We conclude that dual-RNA guided Cas9 cleavage of target DNA is species specific. Depending on the degree of diversity/evolution among Cas9 proteins and tracrRNA:crRNA duplexes, Cas9 and dual-RNA orthologs are partially interchangeable.

Figure S12

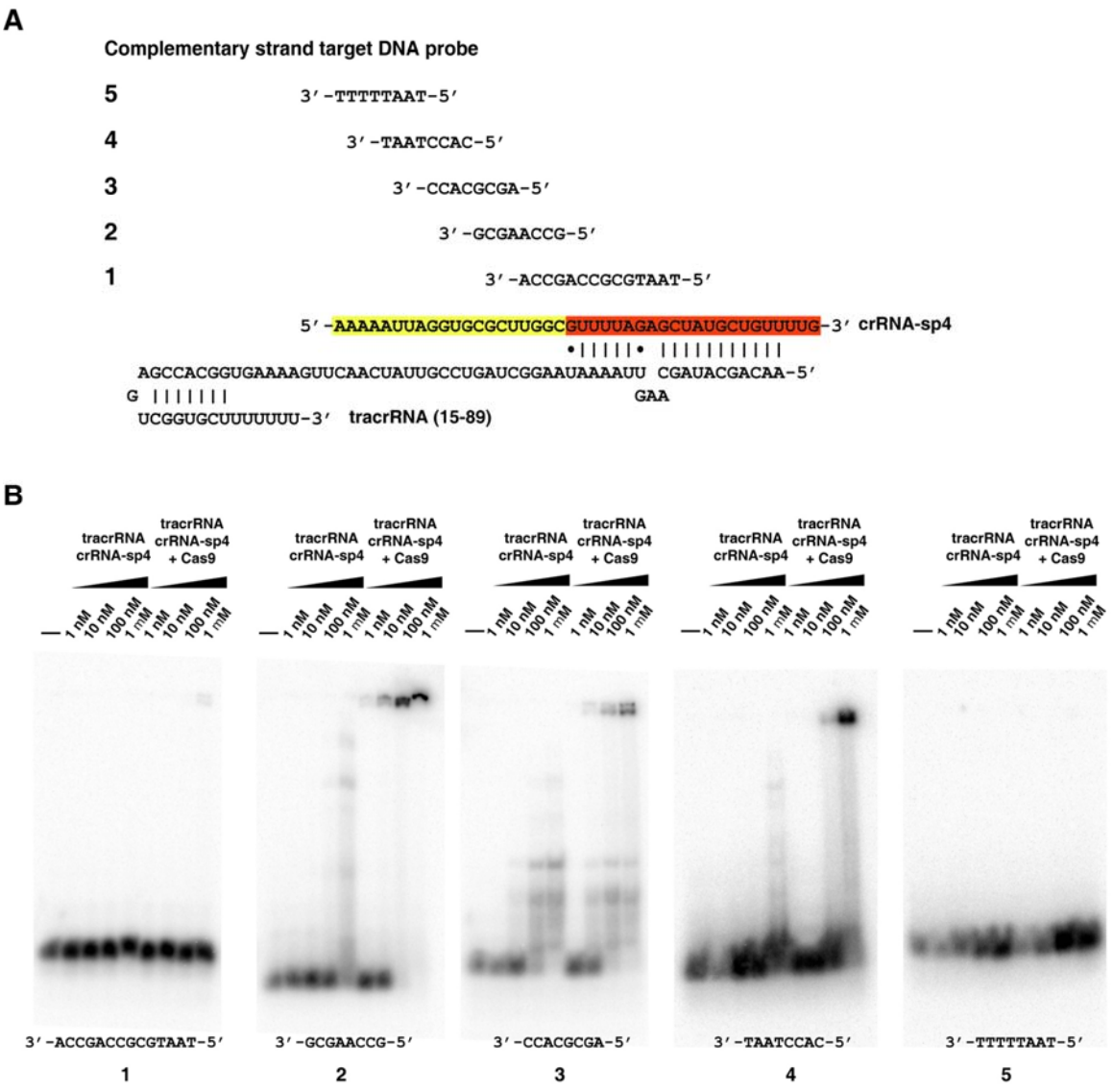

Fig. S12. A seed sequence in the crRNA governs dual tracrRNA:crRNA directed cleavage of target DNA by Cas9. See Fig. 3. A series of 8-nucleotide DNA probes complementary to regions in the crRNA encompassing the DNA-targeting region and tracrRNA-binding region were analyzed for their ability to hybridize to the crRNA in the context of a tracrRNA:crRNA duplex and the Cas9-tracrRNA:crRNA ternary complex. **(A)** Schematic representation of the sequences of DNA probes used in the assay and their binding sites in crRNA-sp4. **(B)** Electrophoretic mobility shift assays of target DNA probes with tracrRNA:crRNA-sp4 or Cas9-tracrRNA:crRNA-sp4. The tracrRNA(15-89) construct was used in the experiment. Binding of the duplexes or complexes to target oligonucleotide DNAs was analyzed on a 16% native polyacrylamide gel and visualized by phosphorimaging.

Figure S13

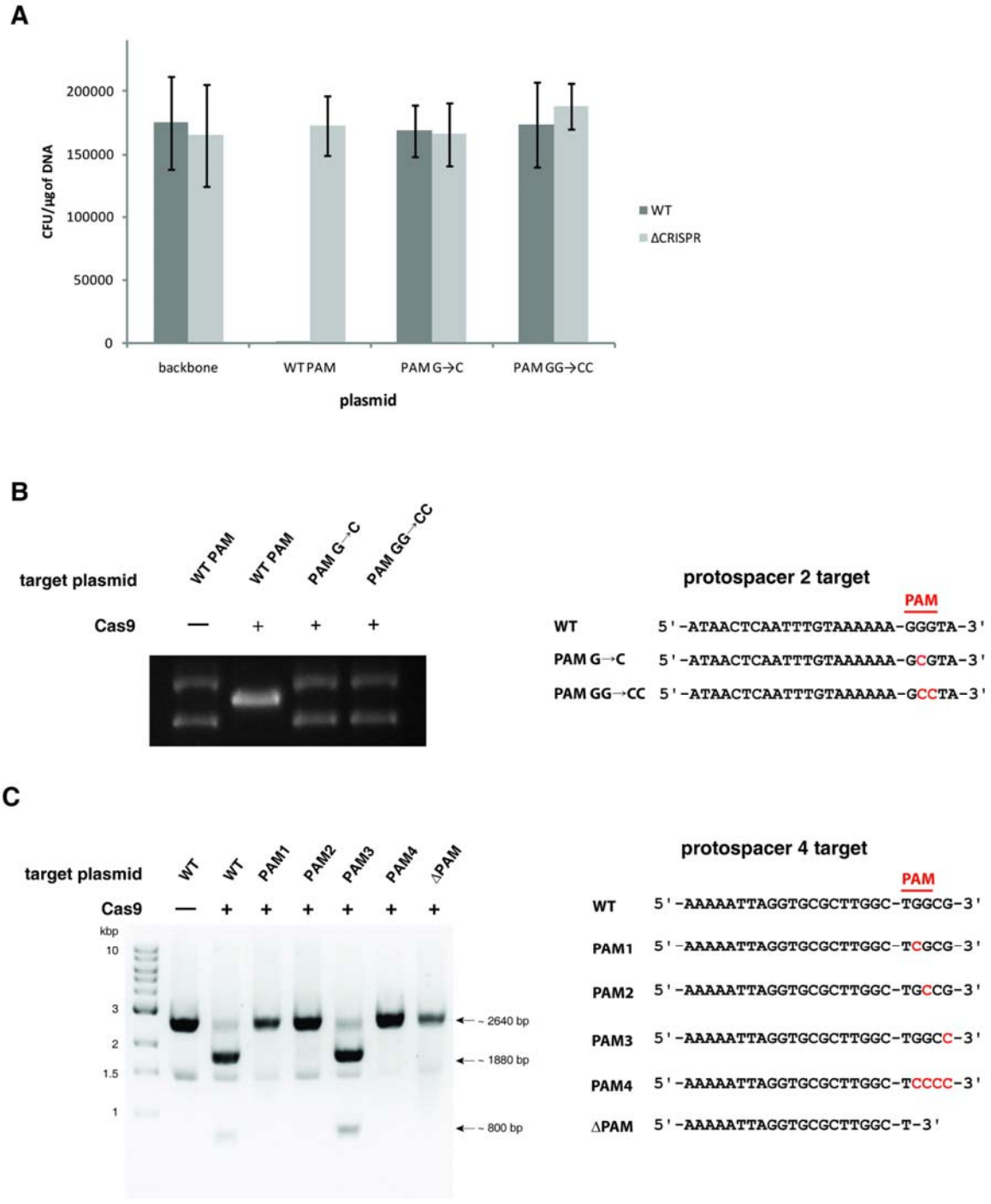

Fig. S13. The PAM sequence is essential for protospacer plasmid DNA cleavage by Cas9-tracrRNA:crRNA and for Cas9-mediated plasmid DNA interference in bacterial cells. See Fig. 4. **(A)** Mutations of the PAM sequence in protospacer 2 plasmid DNA abolish interference of plasmid maintenance by the Type II CRISPR/Cas system in bacterial cells. Wild-type protospacer 2 plasmids with a functional or mutated PAM were transformed into wild-type (strain SF370, also named EC904) and pre-crRNA-deficient mutant (EC1479) *S.*

pyogenes as in Fig. 3D. PAM mutations are not tolerated by the Type II CRISPR/Cas system in vivo. The mean values and standard deviations of three biological replicates are shown. **(B)** Mutations of the PAM sequence in protospacer plasmid DNA abolishes cleavage by Cas9-tracrRNA:crRNA. Wild type protospacer 2 plasmid with a functional or mutated PAM were subjected to Cas9 cleavage as in Fig. 1A. The PAM mutant plasmids are not cleaved by the Cas9-tracrRNA:crRNA complex. **(C)** Mutations of the canonical PAM sequence abolish interference of plasmid maintenance by the Type II CRISPR/Cas system in bacterial cells. Wild-type protospacer 4 plasmids with a functional or mutated PAM were cleaved with Cas9 programmed with tracrRNA and crRNA-sp2. The cleavage reactions were carried out in the presence of the XmnI restriction endonuclease to visualize the Cas9 cleavage products as two fragments (~1880 and ~800 bp). Fragment sizes in base pairs are indicated.

Figure S14

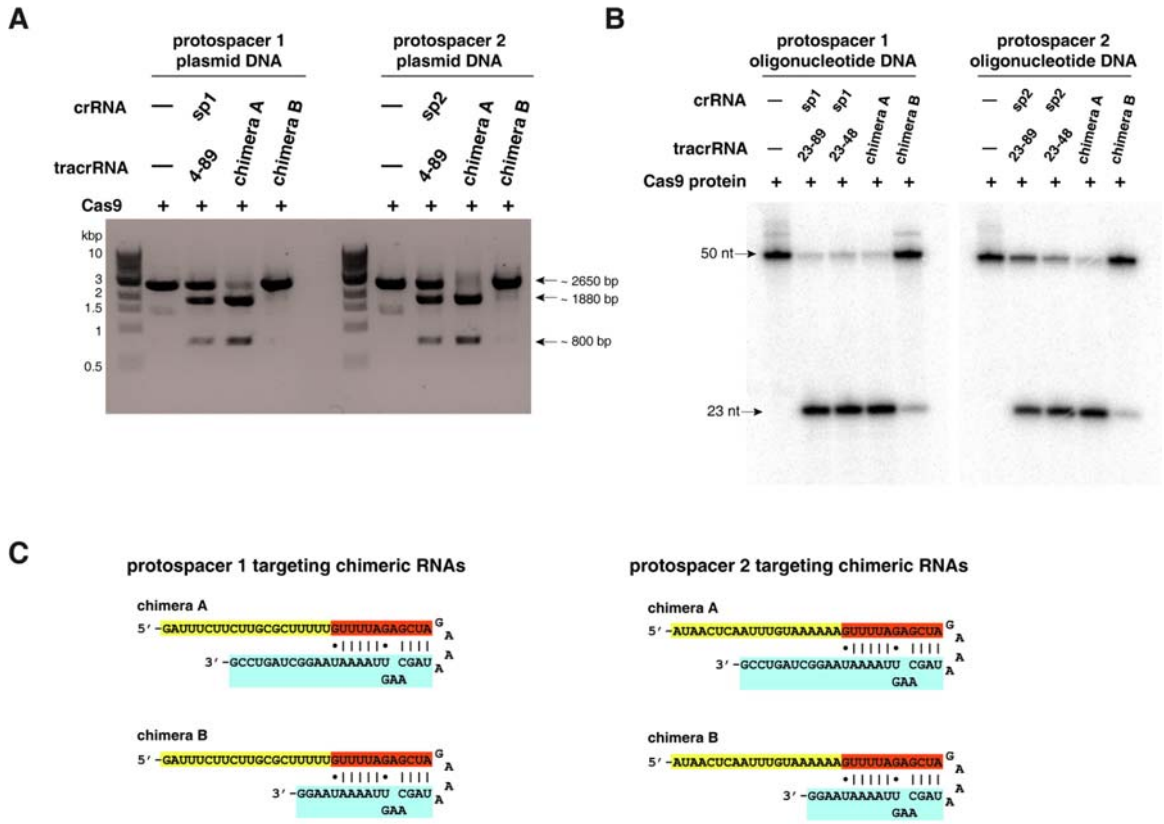

Fig. S14. Cas9 guided by a single chimeric RNA mimicking dual-tracrRNA:crRNA cleaves protospacer DNA. See Fig. 5. **(A)** A single chimeric RNA guides Cas9-catalyzed cleavage of cognate protospacer plasmid DNA (protospacer 1 and protospacer 2). The cleavage reactions were carried out in the presence of the XmnI restriction endonuclease to visualize the Cas9 cleavage products as two fragments (~1880 and ~800 bp). Fragment sizes in base pairs are indicated. **(B)** A single chimeric RNA guides Cas9-catalyzed cleavage of cognate protospacer oligonucleotide DNA (protospacer 1 and protospacer 2). Fragment sizes in nucleotides are indicated. **(C)** Schematic representations of the chimeric RNAs used in the experiment. Sequences of chimeric RNAs A and B are shown with the 5' protospacer DNA-targeting sequence of crRNA (yellow), the tracrRNA-binding sequence of crRNA (orange) and tracrRNA-derived sequence (light blue).

Figure S15

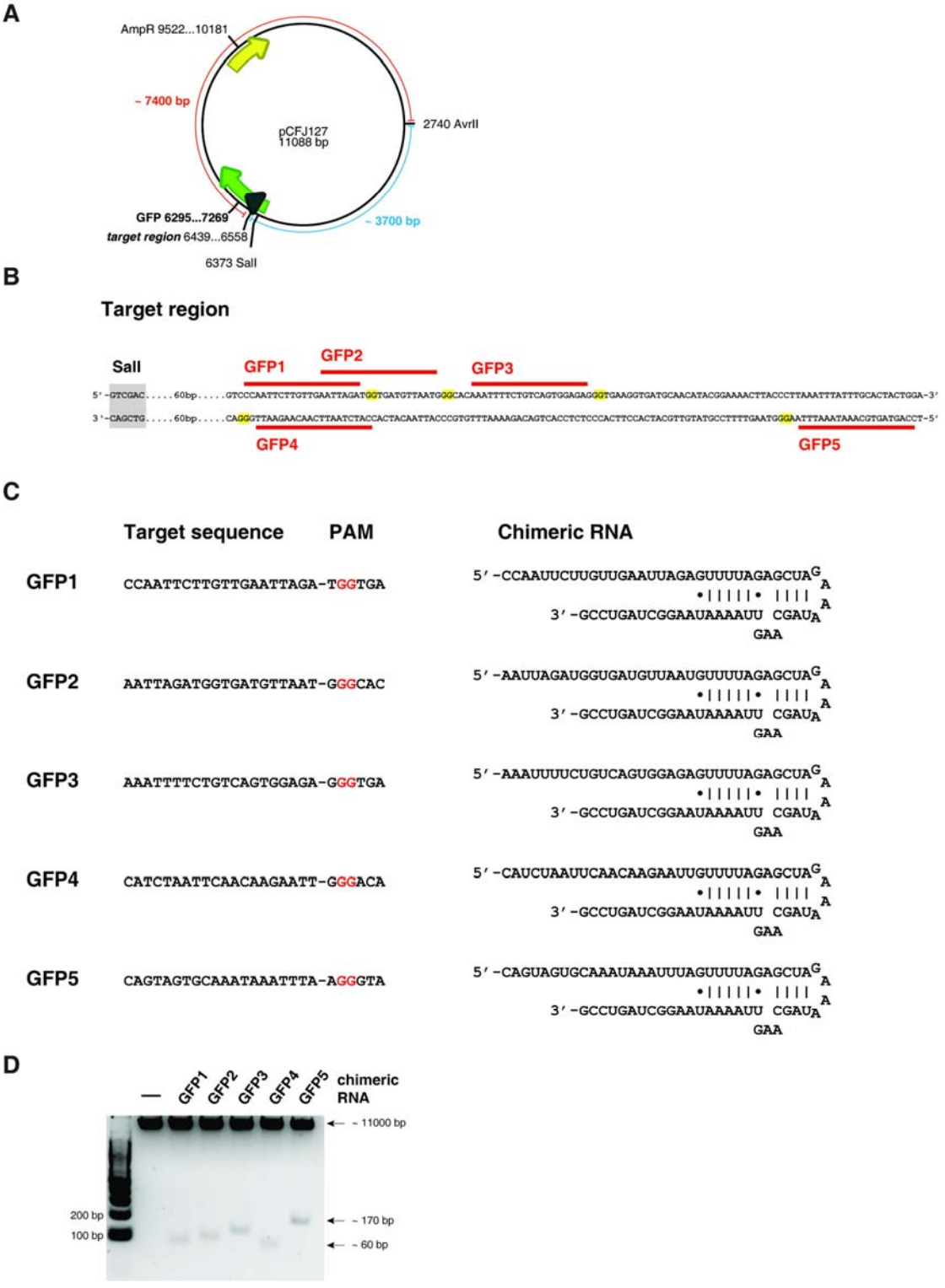

Fig. S15. De novo design of chimeric RNAs targeting the Green Fluorescent Protein (GFP) gene sequence. See Fig. 5. **(A)** Schematic representation of the

GFP expression plasmid pCFJ127. The targeted portion of the GFP open reading frame is indicated with a black arrowhead. **(B)** Close-up of the sequence of the targeted region. Sequences targeted by the chimeric RNAs are shown with red bars. PAM dinucleotides are highlighted in yellow. A unique SalI restriction site is located 60 bp upstream of the target locus. **(C)** Left: Target DNA sequences are shown together with their adjacent PAM motifs. Right: Sequences of the chimeric guide RNAs. **(D)** pCFJ127 was cleaved by Cas9 programmed with chimeric RNAs GFP1-5, as indicated. The plasmid was additionally digested with SalI and the reactions were analyzed by electrophoresis on a 3% agarose gel and visualized by staining with SYBR Safe.

Table S1. Strains used in this study.

Strain	Relevant characteristics	Source
Streptococcus pyogenes		
WT		
EC904	SF370 (M1 serotype)	ATCC 700294
EC1246	MGAS8232 (M18 serotype)	ATCC BAA-572
∆pre-crRNA in SF370		
EC1479	EC904∆pre-crRNA	(*4*)
Campylobacter jejuni		
EC437	NCTC 11168; ATCC 700819 (WT)	CIP 107370
Listeria innocua		
EC917	Clip11262 (WT)	T. Decker
Neisseria meningitides		
Z2491	A Z2491 (WT)	T. Meyer
Streptococcus thermophilus		
EC810	LMD-9 (WT)	P. Renault
Escherichia coli		
RDN204	TOP10, Host for cloning	Invitrogen
BL21 (DE3) Rosetta2	Protein overexpression	Novagen
BL21 (DE3) Rosetta pLysS	Protein overexpression	Novagen

Table S2. Plasmids used in this study.

Plasmids	Relevant characteristics	Source
Vectors for *S. pyogenes*		
pEC85	*repDEG*-pAMβ1, pJH1-*aphIII*, ColE1	Lab plasmid collection
Plasmids for *in vitro* and *in vivo* protospacer assays		
pEC287	pEC85ΩP*speM-speM* (protospacer 2)	Lab plasmid collection
pEC489	pEC85ΩSpy_0700 protospacer 1	Lab plasmid collection
pEC573	pEC85ΩSpy_0700 protospacer 1 (GG PAM)	This study
pEC488	pEC85Ω*speM* protospacer 2	This study
pEC370	pEC488 protospacer 2 mutant A22G	This study
pEC371	pEC488 protospacer 2 mutant T10C	This study
pEC372	pEC488 protospacer 2 mutant T7A	This study
pEC373	pEC488 protospacer 2 mutant A6T	This study
pEC374	pEC488 protospacer 2 mutant A5T	This study
pEC375	pEC488 protospacer 2 mutant A4T	This study
pEC376	pEC488 protospacer 2 mutant A3T	This study
pEC377	pEC488 protospacer 2 PAM mutant G1C	This study
pEC378	pEC488 protospacer 2 PAM mutant GG1,2CC	This study
Plasmids for protospacer cleavage assays		
pMJ849	pUC19 with protospacer 1 and WT PAM inserted between BamHI and EcoRI sites	This study
pMJ850	pUC19 with protospacer 2 and WT PAM inserted between BamHI and EcoRI sites	This study
pMJ852	pUC19 with protospacer 4 and WT PAM inserted between BamHI and EcoRI sites	This study
pMJ856	pUC19 with protospacer 4 and PAM1 mutation inserted between BamHI and EcoRI sites	This study
pMJ857	pUC19 with protospacer 4 and PAM2 mutation inserted between BamHI and EcoRI sites	This study
pMJ858	pUC19 with protospacer 4 and PAM3 mutation inserted between BamHI and EcoRI sites	This study
pMJ859	pUC19 with protospacer 4 and PAM4 mutation inserted between BamHI and EcoRI sites	This study
pMJ860	pUC19 with protospacer 4 and ΔPAM mutation inserted between BamHI and EcoRI sites	This study
pMJ879	pUC19 with protospacer 2 and TGGCG PAM inserted between BamHI and EcoRI sites	This study
pMJ896	pUC19 with protospacer 2 and TGGCG PAM inserted between BamHI and EcoRI sites, nucleotides 19-20 mismatch	This study
pMJ897	pUC19 with protospacer 2 and TGGCG PAM inserted between BamHI and EcoRI sites, nucleotides 17-20 mismatch	This study
pMJ898	pUC19 with protospacer 2 and TGGCG PAM inserted between BamHI and EcoRI sites, nucleotides 15-20 mismatch	This study
pMJ899	pUC19 with protospacer 2 and TGGCG PAM inserted between BamHI and EcoRI sites, nucleotides 13-20 mismatch	This study
pMJ900	pUC19 with protospacer 2 and TGGCG PAM inserted between BamHI and EcoRI sites, nucleotides 11-20 mismatch	This study
pMJ901	pUC19 with protospacer 2 and TGGCG PAM inserted between BamHI and EcoRI sites, nucleotides 9-20 mismatch	This study
pCFJ127	GFP plasmid for cleavage by *de novo* designed RNA chimeras	B. Meyer lab

Plasmids for Cas9 overexpression		
pMJ806	pET-derived His_6-MBP expression vector with *S. pyogenes* Cas9 (1-1368)	This study
pMJ803	pET-derived His_6-MBP expression vector with *C. jejuni* Cas9 (1-984)	This study
pMJ823	pET-derived His_6-Trx expression vector with *L. innocua* Cas9 (1-1334)	This study
pMJ824	pET-derived His_6-GST expression vector with *S. thermophilus* Cas9 (1-1388)	This study
pMJ839	pET-derived His_6-MBP expression vector with *N. meningitidis* Cas9 (1-1082)	This study
pMJ825	pET-derived His_6-MBP expression vector with *S. pyogenes* Cas9 (1-1368), D10A point mutation	This study
pMJ826	pET-derived His_6-MBP expression vector with *S. pyogenes* Cas9 (1-1368), H840A point mutation	This study
pMJ841	pET-derived His_6-MBP expression vector with *S. pyogenes* Cas9 (1-1368), D10A/H840A double mutant	This study

Table S3. Oligonucleotides used in this study.

Oligonucleotides for *in vitro* transcription templates

Purpose	Primer code	Sequence 5'-3'[a]	F/R[b]	Usage
Templates for *in vitro* transcribed CRISPR Type II-A tracrRNA and crRNAs of *S. pyogenes* (for tracrRNA – PCR on chr. DNA SF370; for crRNA – annealing of two oligonucleotides)				
T7-tracrRNA (75nt)	OLEC1521	GAAAT**TAATACGACTCACTATAG***AAAACAGCATAGCA AGTTAAAATAA*	F	5' tracrRNA
	OLEC1522	*AAAAAAAGCACCGACTCGGTGCCAC*	R	3' tracrRNA
T7-crRNA (template)	OLEC2176	GAAAT**TAATACGACTCACTATAGG**GATTTCTTCTTGC GCTTTTTGTTTTAGAGCTATGCTGTTTTG	F	crRNA-sp1
	OLEC2178	CAAAACAGCATAGCTCTAAAACAAAAAGCGCAAGAAG AAATC**CCTATAGTGAGTCGTATTA**ATTTC	R	crRNA-sp1
	OLEC2177	GAAAT**TAATACGACTCACTATAGG**ATAACTCAATTTG TAAAAAAGTTTTAGAGCTATGCTGTTTTG	F	crRNA-sp2
	OLEC2179	CAAAACAGCATAGCTCTAAAACTTTTTTACAAATTGAG TTAT**CCTATAGTGAGTCGTATTA**ATTTC	R	crRNA-sp2
Templates for *in vitro* transcribed *N. meningitidis* tracrRNA and engineered crRNA-sp2 (for tracrRNA – PCR on chr. DNA Z2491; for crRNA – annealing of two oligonucleotides)				
T7-tracrRNA	OLEC2205	GAAAT**TAATACGACTCACTATAGATG***ATGAGAACCG TTGCTACAATAAGGC*	F	Predicted 5'
	OLEC2206	*AAATAAACGATGCCCCTTAAAGCA*	R	Predicted 3'
T7-crRNA (template)	OLEC2209	GAAAT**TAATACGACTCACTATAGATG**ATAACTCAATT TGTAAAAAAGTTGTAGCTCCCTTTCTCATTT	F	sp2(*speM*) + *N.m.* repeat
	OLEC2214	AAATGAGAAAGGGAGCTACAACTTTTTTACAAATTGA GTTATC**ATCTATAGTGAGTCGTATTA**ATTTC	R	sp2(*speM*) + *N.m.* repeat
Templates for *in vitro* transcribed *L. innocua* tracrRNA and engineered crRNA-sp2 (for tracrRNA – PCR on chr. DNA Clip11262; for crRNA – annealing of two oligonucleotides)				
T7-tracrRNA	OLEC2203	GAAAT**TAATACGACTCACTATAGATG***AAATAACATAG CAAGTTAAAATAAG*	F	Predicted 5'
	OLEC2204	*AAAAAAAGCGCCGAAACAGCGCTACTTAATT*	R	Predicted 3'
T7-crRNA (template)	OLEC2207	GAAAT**TAATACGACTCACTATAGATG**ATAACTCAATT TGTAAAAAAGTTTTAGAGCTATGTTATTTTG	F	sp2(*speM*) + *L. in.* repeat
	OLEC2212	CAAAATAACATAGCTCTAAAACTTTTTTACAAATTGAG TTATC**ATCTATAGTGAGTCGTATTA**ATTTC	R	sp2(*speM*) + *L.in.* repeat

Oligonucleotides for constructing plasmids with protospacer for in vitro and in vivo studies

Purpose	Primer code	Sequence 5'-3'[a]	F/R[b]	Usage
Plasmids for *speM* (spacer 2 (CRISPR Type II-A, SF370; protospacer prophage ø8232.3 from MGAS8232) analysis *in vitro* and in *S. pyogenes* (template: chr. DNA MGAS8232 or plasmids containing *speM* fragments)				
pEC287	OLEC1555	ATGCACCTGCAG*GATGCTGTTAAATAATTGTATAC*	F	P*speM*
	OLEC1556	ATGCACGGATCC*AGCTGCTCTAAGTCTACTAAAACC*	R	*speM*
pEC488	OLEC2145	ATGCAGGGCCGGCC*GTGACAGAGAGAAACTTGATTC AAC*	F	*speM*
	OLEC2146	ATGCAGGGCCGGCC*CTTCGTTTAAGTAAACATCAAAG TG*	R	*speM*
pEC370	OLEC1593	*ATGAGCGATAATAGAATAAAGTTATATGAGCATAACT CAATTTGTAAAAAAGGGTATTG*	F	pEC488 protospacer 2 A22G
	OLEC1594	*CAATACCCTTTTTTACAAATTGAGTTATGCTCATATAA CTTTATTCTATTATCGCTCAT*	R	
pEC371	OLEC1595	*GCGATAATAGAATAAAGTTATATGAACATAACTCAATC TGTAAAAAAGGGTATTGGG*	F	pEC488 protospacer 2 T10C
	OLEC1596	*CCCAATACCCTTTTTTACAGATTGAGTTATGTTCATAT AACTTTATTCTATTATCGC*	R	
pEC372	OLEC2185	*GAACATAACTCAATTTGAAAAAAAGGGTATTGGGGAA TTC*	F	pEC488 protospacer 2 T7A
	OLEC2186	*GAATTCCCCAATACCCTTTTTTTCAAATTGAGTTATGT TC*	R	

pEC373	OLEC2187	*GAACATAACTCAATTTGT*TAAAAAGGGTATTGGGGAA*TTC*	F	pEC488 protospacer 2 A6T
	OLEC2188	*GAATTCCCCAATACCCTTTTT*AACAAATTGAGTTATGT*TC*	R	
pEC374	OLEC2235	*GAACATAACTCAATTTGTA*TAAAAGGGTATTGGGGAA*TTCATT*	F	pEC488 protospacer 2 A5T
	OLEC2236	*AATGAATTCCCCAATACCCTTTTATACAAATTGAGTTA TGTTC*	R	
pEC375	OLEC2233	*GAACATAACTCAATTTGTAA*TAAAGGGTATTGGGGAA*TTCATT*	F	pEC488 protospacer 2 A4T
	OLEC2234	*AATGAATTCCCCAATACCCTTTATTACAAATTGAGTTA TGTTC*	R	
pEC376	OLEC2189	*CATAACTCAATTTGTAAA*TAAGGGTATTGGGGAATTC*ATT*	F	pEC488 protospacer 2 A3T
	OLEC2190	*AATGAATTCCCCAATACCCTTATTTACAAATTGAGTTA TG*	R	
pEC377	OLEC2191	*CATAACTCAATTTGTAAAAAAG*CGTATTGGGGAATTC*ATTATAAAG*	F	pEC488 protospacer 2 PAM G1C
	OLEC2192	*CTTTATAATGAATTCCCCAATAC*GCTTTTTTACAAATT*GAGTTATG*	R	
pEC378	OLEC2237	*CATAACTCAATTTGTAAAAAAG*CC*TATTGGGGAATTCA TTATAA*	F	pEC488 protospacer 2 PAM GG1,2CC
	OLEC2238	*TTATAATGAATTCCCCAATA*GG*CTTTTTTACAAATTGA GTTATG*	R	
Plasmids for SPy_0700 (spacer 1 (CRISPR Type II-A, SF370; protospacer prophage ø370.1 from SF370) analysis *in vitro* and in *S. pyogenes* (template: chr. DNA SF370 or plasmids containing SPy_0700 fragments)				
pEC489	OLEC2106	ATGCAG<u>GGCCGGCC</u>*AGTATCAGCGTACTTGGATTTG GG*	F	Spy_0700
	OLEC2107	ATGCAG<u>GGCCGGCC</u>*TTGTCTCACTCACTCTATTTTTG*	R	Spy_0700
pEC573	OLEC2941	*GATTTCTTGCGCTTTTTTGGCTTTTTCGAG*	F	PAM TG1,2GG
	OLEC2942	*GGGATGGCAATCCATGGGTCAAGGTACTAG*	R	

Oligonucleotides for verification of plasmid constructs and cutting sites by sequencing analysis.

ColE1 (pEC85)	oliRN228	*GGAACGAAAACTCACGTTAA*	R	sequencing
speM (pEC287)	OLEC1557	*TGAGAGTGTCTTTTCAGATGCTGTG*	F	sequencing
	OLEC1556	*AGCGGTATCTGTTCCCCAAAA*	R	sequencing
repDEG-pAMbeta1 (pEC85)	OLEC787	*GTTAAAAACCACGTAACCACA*	F	sequencing

[a] *italic*, sequence annealing to the template; <u>underlined</u>, restriction site; **bold**, T7 promoter.
[b] F, forward primer; R, reverse primer.

Oligonucleotides for *in vitro* cleavage assays.

Purpose	Sequence 5'-3'
crRNA	
Spacer 1 crRNA (1-42)	GAUUUCUUCUUGCGCUUUUUGUUUUAGAGCUAUGCUGUUUUG
Spacer 2 crRNA (1-42)	AUAACUCAAUUUGUAAAAAAGUUUUAGAGCUAUGCUGUUUUG
Spacer 4 crRNA (1-42)	AAAAAUUAGGUGCGCUUGGCGUUUUAGAGCUAUGCUGUUUUG
Spacer 2 crRNA (1-36)	AUAACUCAAUUUGUAAAAAAGUUUUAGAGCUAUGCU
Spacer 2 crRNA (1-32)	AUAACUCAAUUUGUAAAAAAGUUUUAGAGCUA
Spacer 2 crRNA (11-42)	UUGUAAAAAAGUUUUAGAGCUA
tracrRNA	
(4-89)	GUUGGAACCAUUCAAAACAGCAUAGCAAGUUAAAAUAAGGCUAGUCCGUUAUCAACUUGAAAAAGUGGCACCGAGUCGGUGCUUUUUUU
(15-89)	AACAGCAUAGCAAGUUAAAAUAAGGCUAGUCCGUUAUCAACUUGAAAAAGUGGCACCGAGUCGGUGCUUUUUUU
(23-89)	UAGCAAGUUAAAAUAAGGCUAGUCCGUUAUCAACUUGAAAAAGUGGCACCGAGUCGGUGCUUUUUUU

Purpose	Sequence 5'-3'
tracrRNA continued	
(15-53)	AAACAGCAUAGCAAGUUAAAAUAAGGCUAGUCCGUUAUC
(15-44)	AAACAGCAUAGCAAGUUAAAAUAAGGCUAG
(15-36)	AAACAGCAUAGCAAGUUAAAAU
(23-53)	UAGCAAGUUAAAAUAAGGCUAGUCCGUUAUC
(23-48)	UAGCAAGUUAAAAUAAGGCUAGUCCG
(23-44)	UAGCAAGUUAAAAUAAGGCUAG
(1-26)	GUUGGAACCAUUCAAAACAGCAUAGC
chimeric RNAs	**(targeting sequence shown in bold)**
Spacer 1 – chimera A	**GAUUUCUUCUUGCGCUUUUU**GUUUUAGAGCUAGAAAUAGCAAGUUAAAAUAAGGC UAGUCCG
Spacer 1 – chimera B	**GAUUUCUUCUUGCGCUUUUU**GUUUUAGAGCUAGAAAUAGCAAGUUAAAAUAAGG
Spacer 2 – chimera A	**AUAACUCAAUUUGUAAAAAA**GUUUUAGAGCUAGAAAUAGCAAGUUAAAAUAAGGC UAGUCCG
Spacer 2 – chimera B	**AUAACUCAAUUUGUAAAAAA**GUUUUAGAGCUAGAAAUAGCAAGUUAAAAUAAGG
Spacer 4 – chimera A	**AAAAAUUAGGUGCGCUUGGC**GUUUUAGAGCUAGAAAUAGCAAGUUAAAAUAAGGC UAGUCCG
Spacer 4 – chimera B	**AAAAAUUAGGUGCGCUUGGC**GUUUUAGAGCUAGAAAUAGCAAGUUAAAAUAAGG
GFP1	**CCAATTCTTGTTGAATTAGA**GUUUUAGAGCUAGAAAUAGCAAGUUAAAAUAAGGCUA GUCCG
GFP2	**AATTAGATGGTGATGTTAAT**GUUUUAGAGCUAGAAAUAGCAAGUUAAAAUAAGGCU AGUCCG
GFP3	**AAATTTTCTGTCAGTGGAGA**GUUUUAGAGCUAGAAAUAGCAAGUUAAAAUAAGGCU AGUCCG
GFP4	**CATCTAATTCAACAAGAATT**GUUUUAGAGCUAGAAAUAGCAAGUUAAAAUAAGGCU AGUCCG
GFP5	**CAGTAGTGCAAATAAATTTA**GUUUUAGAGCUAGAAAUAGCAAGUUAAAAUAAGGCU AGCCG
DNA oligonucleotides as substrates for cleavage assays (protospacer in bold, PAM underlined)	
protospacer 1 - complementary – WT	TAATGAATTCCCCAATACCC**AAAAAGCGCAAGAAGAAATC**AACCAGCGCA
protospacer 1 - noncomplementary – WT	TGCGCTGGTT**GATTTCTTCTTGCGCTTTTT**GGGTATTGGGGAATTCATTA
protospacer 2 - complementary – WT	TAATGAATTCCCCAATACCC**TTTTTTACAAATTGAGTTAT**GTTCATATAA
protospacer 2 - noncomplementary – WT	TTATATGAAC**ATAACTCAATTTGTAAAAAA**GGGTATTGGGGAATTCATTA
protospacer 4 - complementary – WT	TAATGCGCCA**GCCAAGCGCACCTAATTTTT**CCTCGGCACTTAATATAACC
protospacer 4 - noncomplementary – WT	GGTTATATTAAGTGCCGAGG**AAAAATTAGGTGCGCTTGGC**TGGCGCATTA
protospacer 2 - complementary - PAM1	TAATGAATTCCCCAATAGGC**TTTTTTACAAATTGAGTTAT**GTTCATATAA
protospacer 2 - noncomplementary - PAM1	TTATATGAAC**ATAACTCAATTTGTAAAAAA**GCCTATTGGGGAATTCATTA
protospacer 2 - complementary - PAM2	TAATGAATTCCCGTTATGGC**TTTTTTACAAATTGAGTTAT**GTTCATATAA
protospacer 2 - noncomplementary - PAM2	TTATATGAAC**ATAACTCAATTTGTAAAAAA**GCCATAACGGGAATTCATTA
protospacer 4 - complementary - PAM1	TAATGCGCGA**GCCAAGCGCACCTAATTTTT**CCTCGGCACTTAATATAACC
protospacer 4 - noncomplementary - PAM1	GGTTATATTAAGTGCCGAGG**AAAAATTAGGTGCGCTTGGC**TCGCGCATTA
protospacer 4 - complementary - PAM2	TAATGCGGCA**GCCAAGCGCACCTAATTTTT**CCTCGGCACTTAATATAACC
protospacer 4 - noncomplementary - PAM2	GGTTATATTAAGTGCCGAGG**AAAAATTAGGTGCGCTTGGC**TGCCGCATTA

References and Notes

1. B. Wiedenheft, S. H. Sternberg, J. A. Doudna, RNA-guided genetic silencing systems in bacteria and archaea. *Nature* **482**, 331 (2012). doi:10.1038/nature10886 Medline

2. D. Bhaya, M. Davison, R. Barrangou, CRISPR-Cas systems in bacteria and archaea: Versatile small RNAs for adaptive defense and regulation. *Annu. Rev. Genet.* **45**, 273 (2011). doi:10.1146/annurev-genet-110410-132430 Medline

3. M. P. Terns, R. M. Terns, CRISPR-based adaptive immune systems. *Curr. Opin. Microbiol.* **14**, 321 (2011). doi:10.1016/j.mib.2011.03.005 Medline

4. E. Deltcheva *et al*., CRISPR RNA maturation by trans-encoded small RNA and host factor RNase III. *Nature* **471**, 602 (2011). doi:10.1038/nature09886 Medline

5. J. Carte, R. Wang, H. Li, R. M. Terns, M. P. Terns, Cas6 is an endoribonuclease that generates guide RNAs for invader defense in prokaryotes. *Genes Dev.* **22**, 3489 (2008). doi:10.1101/gad.1742908 Medline

6. R. E. Haurwitz, M. Jinek, B. Wiedenheft, K. Zhou, J. A. Doudna, Sequence- and structure-specific RNA processing by a CRISPR endonuclease. *Science* **329**, 1355 (2010). doi:10.1126/science.1192272 Medline

7. R. Wang, G. Preamplume, M. P. Terns, R. M. Terns, H. Li, Interaction of the Cas6 riboendonuclease with CRISPR RNAs: Recognition and cleavage. *Structure* **19**, 257 (2011). Medline

8. E. M. Gesner, M. J. Schellenberg, E. L. Garside, M. M. George, A. M. Macmillan, Recognition and maturation of effector RNAs in a CRISPR interference pathway. *Nat. Struct. Mol. Biol.* **18**, 688 (2011). doi:10.1038/nsmb.2042 Medline

9. A. Hatoum-Aslan, I. Maniv, L. A. Marraffini, Mature clustered, regularly interspaced, short palindromic repeats RNA (crRNA) length is measured by a ruler mechanism anchored at the precursor processing site. *Proc. Natl. Acad. Sci. U.S.A.* **108**, 21218 (2011). doi:10.1073/pnas.1112832108 Medline

10. S. J. J. Brouns *et al*., Small CRISPR RNAs guide antiviral defense in prokaryotes. *Science* **321**, 960 (2008). doi:10.1126/science.1159689 Medline

11. D. G. Sashital, M. Jinek, J. A. Doudna, An RNA-induced conformational change required for CRISPR RNA cleavage by the endoribonuclease Cse3. *Nat. Struct. Mol. Biol.* **18**, 680 (2011). doi:10.1038/nsmb.2043 Medline

12. N. G. Lintner *et al*., Structural and functional characterization of an archaeal clustered regularly interspaced short palindromic repeat (CRISPR)-associated complex for antiviral defense (CASCADE). *J. Biol. Chem.* **286**, 21643 (2011). doi:10.1074/jbc.M111.238485 Medline

13. E. Semenova *et al*., Interference by clustered regularly interspaced short palindromic repeat (CRISPR) RNA is governed by a seed sequence. *Proc. Natl. Acad. Sci. U.S.A.* **108**, 10098 (2011). doi:10.1073/pnas.1104144108 Medline

14. B. Wiedenheft *et al*., RNA-guided complex from a bacterial immune system enhances target recognition through seed sequence interactions. *Proc. Natl. Acad. Sci. U.S.A.* **108**, 10092 (2011). doi:10.1073/pnas.1102716108 Medline

15. B. Wiedenheft *et al*., Structures of the RNA-guided surveillance complex from a bacterial immune system. *Nature* **477**, 486 (2011). doi:10.1038/nature10402 Medline

16. C. R. Hale *et al*., RNA-guided RNA cleavage by a CRISPR RNA-Cas protein complex. *Cell* **139**, 945 (2009). doi:10.1016/j.cell.2009.07.040 Medline

17. J. A. L. Howard, S. Delmas, I. Ivančić-Baće, E. L. Bolt, Helicase dissociation and annealing of RNA-DNA hybrids by *Escherichia coli* Cas3 protein. *Biochem. J.* **439**, 85 (2011). doi:10.1042/BJ20110901 Medline

18. E. R. Westra *et al*., CRISPR immunity relies on the consecutive binding and degradation of negatively supercoiled invader DNA by Cascade and Cas3. *Mol. Cell* **46**, 595 (2012). doi:10.1016/j.molcel.2012.03.018 Medline

19. C. R. Hale *et al*., Essential features and rational design of CRISPR RNAs that function with the Cas RAMP module complex to cleave RNAs. *Mol. Cell* **45**, 292 (2012). doi:10.1016/j.molcel.2011.10.023 Medline

20. J. Zhang *et al*., Structure and mechanism of the CMR complex for CRISPR-mediated antiviral immunity. *Mol. Cell* **45**, 303 (2012). doi:10.1016/j.molcel.2011.12.013 Medline

21. K. S. Makarova *et al*., Evolution and classification of the CRISPR-Cas systems. *Nat. Rev. Microbiol.* **9**, 467 (2011). doi:10.1038/nrmicro2577 Medline

22. K. S. Makarova, N. V. Grishin, S. A. Shabalina, Y. I. Wolf, E. V. Koonin, A putative RNA-interference-based immune system in prokaryotes: Computational analysis of the predicted enzymatic machinery, functional analogies with eukaryotic RNAi, and hypothetical mechanisms of action. *Biol. Direct* **1**, 7 (2006). doi:10.1186/1745-6150-1-7 Medline

23. K. S. Makarova, L. Aravind, Y. I. Wolf, E. V. Koonin, Unification of Cas protein families and a simple scenario for the origin and evolution of CRISPR-Cas systems. *Biol. Direct* **6**, 38 (2011). doi:10.1186/1745-6150-6-38 Medline

24. S. Gottesman, Microbiology: Dicing defence in bacteria. *Nature* **471**, 588 (2011). doi:10.1038/471588a Medline

25. R. Barrangou *et al*., CRISPR provides acquired resistance against viruses in prokaryotes. *Science* **315**, 1709 (2007). doi:10.1126/science.1138140 Medline

26. J. E. Garneau *et al*., The CRISPR/Cas bacterial immune system cleaves bacteriophage and plasmid DNA. *Nature* **468**, 67 (2010). doi:10.1038/nature09523 Medline

27. R. Sapranauskas *et al*., The *Streptococcus thermophilus* CRISPR/Cas system provides immunity in *Escherichia coli*. *Nucleic Acids Res.* **39**, 9275 (2011). doi:10.1093/nar/gkr606 Medline

28. G. K. Taylor, D. F. Heiter, S. Pietrokovski, B. L. Stoddard, Activity, specificity and structure of I-Bth0305I: A representative of a new homing endonuclease family. *Nucleic Acids Res.* **39**, 9705 (2011). doi:10.1093/nar/gkr669 Medline

29. H. Deveau *et al*., Phage response to CRISPR-encoded resistance in *Streptococcus thermophilus*. *J. Bacteriol.* **190**, 1390 (2008). doi:10.1128/JB.01412-07 Medline

30. B. P. Lewis, C. B. Burge, D. P. Bartel, Conserved seed pairing, often flanked by adenosines, indicates that thousands of human genes are microRNA targets. *Cell* **120**, 15 (2005). doi:10.1016/j.cell.2004.12.035 Medline

31. G. Hutvagner, M. J. Simard, Argonaute proteins: Key players in RNA silencing. *Nat. Rev. Mol. Cell Biol.* **9**, 22 (2008). doi:10.1038/nrm2321 Medline

32. F. J. M. Mojica, C. Díez-Villaseñor, J. García-Martínez, C. Almendros, Short motif sequences determine the targets of the prokaryotic CRISPR defence system. *Microbiology* **155**, 733 (2009). doi:10.1099/mic.0.023960-0 Medline

33. L. A. Marraffini, E. J. Sontheimer, Self versus non-self discrimination during CRISPR RNA-directed immunity. *Nature* **463**, 568 (2010). doi:10.1038/nature08703 Medline

34. D. G. Sashital, B. Wiedenheft, J. A. Doudna, Mechanism of foreign DNA selection in a bacterial adaptive immune system. *Mol. Cell* **46**, 606 (2012). doi:10.1016/j.molcel.2012.03.020 Medline

35. M. Christian *et al*., Targeting DNA double-strand breaks with TAL effector nucleases. *Genetics* **186**, 757 (2010). doi:10.1534/genetics.110.120717 Medline

36. J. C. Miller *et al*., A TALE nuclease architecture for efficient genome editing. *Nat. Biotechnol.* **29**, 143 (2011). doi:10.1038/nbt.1755 Medline

37. F. D. Urnov, E. J. Rebar, M. C. Holmes, H. S. Zhang, P. D. Gregory, Genome editing with engineered zinc finger nucleases. *Nat. Rev. Genet.* **11**, 636 (2010). doi:10.1038/nrg2842 Medline

38. D. Carroll, Progress and prospects: zinc-finger nucleases as gene therapy agents. *Gene Ther.* **15**, 1463 (2008). doi:10.1038/gt.2008.145 Medline

39. J. Sambrook, E. F. Fritsch, T. Maniatis, *Molecular Cloning: A Laboratory Manual* (Cold Spring Harbor Laboratory Press, Cold Spring Harbor, NY, ed. 2, 1989).

40. M. G. Caparon, J. R. Scott, Genetic manipulation of pathogenic streptococci. *Methods Enzymol.* **204**, 556 (1991). doi:10.1016/0076-6879(91)04028-M Medline

41. C. Frøkjær-Jensen *et al*., Single-copy insertion of transgenes in *Caenorhabditis elegans*. *Nat. Genet.* **40**, 1375 (2008). doi:10.1038/ng.248 Medline

42. R. B. Denman, Using RNAFOLD to predict the activity of small catalytic RNAs. *Biotechniques* **15**, 1090 (1993). Medline

43. I. L. Hofacker, P. F. Stadler, Memory efficient folding algorithms for circular RNA secondary structures. *Bioinformatics* **22**, 1172 (2006). doi:10.1093/bioinformatics/btl023 Medline

44. K. Darty, A. Denise, Y. Ponty, VARNA: Interactive drawing and editing of the RNA secondary structure. *Bioinformatics* **25**, 1974 (2009). doi:10.1093/bioinformatics/btp250 Medline

45. J. A. Zebala, J. Choi, F. Barany, Characterization of steady state, single-turnover, and binding kinetics of the TaqI restriction endonuclease. *J. Biol. Chem.* **267**, 8097 (1992). Medline

46. V. Pingoud *et al*., On the divalent metal ion dependence of DNA cleavage by restriction endonucleases of the EcoRI family. *J. Mol. Biol.* **393**, 140 (2009). doi:10.1016/j.jmb.2009.08.011 Medline

47. D. J. Wright, W. E. Jack, P. Modrich, The kinetic mechanism of EcoRI endonuclease. *J. Biol. Chem.* **274**, 31896 (1999). doi:10.1074/jbc.274.45.31896 Medline